or ductular structures also increases. In contrast, PT ductular reaction is present even in low stage biopsies and the degree of ductular reaction does not correlate well with stage.

	Centrilobular Zone				Portal Tracts		
	No CK7+ cells (%)	Single CK7+ cells (%)	Strings of CK7+ cells (%)	CK7+ ductules (%)	No ductular reaction (%)	Mild ductular reaction (%)	Florid ductular reaction (%)
Stage 0	82.6	17.1	0.4	0	33.0	52.8	14.1
Stage 1	73.2	20.9	3.0	3.0	26.3	52.9	20.8
Stage 2	54.2	23.2	14.3	8.3	23.2	62.1	15.3
Stage3	33.7	26.6	22.9	16.8	8.2	60.0	32.1
p value	<0.0001	0.54	0.0009	0.008	0.072	0.78	0.042

Conclusions: CK7+ CLZ ductular elements are common in NASH and their development correlates with increasing fibrosis stage. The presence of CLZ CK7+ ductular elements can cause confusion in distinguishing PTs from CLZs and GS stains can be helpful in this regard by highlighting CLZs. It is possible that the development of the CLZ ductular reaction contributes to the development of fibrosis in NASH. If so, scoring of CK7+ ductular elements would be a useful addition to the schema for GRADING in NASH.

1774 Abnormal Hepatocellular Mitochondria in Methylmalonic Acidemia

J Ziskin, Y Wilnai, G Enns, A-K Niemi, H Vogel. Stanford University, Palo Alto, CA.

Background: Methylmalonic acidemia (MMA) is one of the most frequently encountered forms of branched-chain organic acidemias. Biochemical abnormalities seen in some MMA patients, such as lactic acidemia and increased TCA cycle intermediate excretion, suggest mitochondrial dysfunction.

Design: In order to investigate the possibility of mitochondrial involvement in MMA, we examined the livers from patients with mutations that cause complete absence of methylmalonyl CoA mutase enzyme activity (MMA *mut^0*). .Biopsies from five explanted livers from MMA *mut^0* patients undergoing liver transplantation were evaluated for mitochondrial ultrastructural abnormalities. The patients ranged from 10 months to 17 years of age and all patients had previous episodes of metabolic acidosis, lactic acidemia, ketonuria and hyperammonemia.

Results: All biopsies revealed a striking mitochondriopathy by electron microscopy that were not found in control pediatric liver biopsies. Mitochondria were markedly variable in size, shape, and conformation of cristae. The inner matrix appeared to be greatly expanded and the cristae were diminutive and disconnected. No crystalloid inclusions were noted.

Conclusions: This study clearly documents extensive mitochondrial ultrastructure abnormalities in all liver samples in this series from MMA *mut^0* patients undergoing transplantation, providing pathological evidence for mitochondrial dysfunction in the pathophysiology of methylmalonyl CoA mutase enzyme inactivity. This series suggests that future studies are warranted in patients with alternative mutations in methylmalyonyl CoA mutase and patients with mutations in alternative genes associated with MMA, such as *MMAA*, *MMAB*, and *MMADHC* genes, in order to elucidate the prevalence and role of mitochondrial dysfunction across these diverse genetic causes. The marked enlargement of mitochondria in these cases may indicate a perturbation in mitochondrial fission in MMA. The correlation between mitochondrial dysfunction and morphological abnormalities in MMA may provide insights for better understanding and monitoring of optimized or novel therapeutic strategies.

Neuropathology

1775 Clinical Molecular Staging in Meningiomas: Prospective Experience of a Single Institution Using Routine FFPE Samples

MS Abedalthagafi, SH Ramkissoon, KL Ligon, AH Ligon, RD Folkerth, S Santagata. Brigham and Women's Hospital and Harvard Medical School, Boston, MA.

Background: Meningiomas are the most common primary intracranial tumors, and are clinically, histologically and molecularly heterogeneous. They are classified into the three World Health Organization grades: I (benign), II (atypical) and III (anaplastic). Several copy number variations (CNVs) have been suggested as prognostic factors, but real time molecular signatures using aCGH have never been used in routine clinical practice.

Design: We developed an array comparative genomic hybridization (aCGH) method to assess copy number changes in FFPE tissues (Craig JM., et al., PLoS One. 2012; 7(6):e38881). We performed aCGH on unselected 116 meningiomas received during a thirteenth-month period to test the hypothesis that different grades have different CNV signatures. Copy number aberrations were correlated further with clinical data.

Results: In addition to the known CNVs in the WHO classifications, we identified several new molecular signatures including: single copy loss in 12q , polysomy in chromosomes 3, 4, 5, 6, 7, 9, 13, 16, 18, 19, 20 and 21, occurring singly or in combination, in our sample. Three WHO grade I meningiomas with brain invasion, but insufficient WHO features of atypia, had grade II genomic signatures. Our genomic approach also led to the histologic re-classification of two uncertain "poorly differentiated neoplasms" into anaplastic meningioma.

WHO grade	22q- and/or 1p-	mono6 and/ or 6q-	Significant Others
I (n=65)*	36 (55.3 % of have 22q- , 27% have 22q- and 1p-)	6 (9.3%)	Trisomy 1,2,3,5,9,10,12,13,15,18,20,21 5(7.69%)
II (n=37)	25 (67.5%)	8(21.6%)	-3P,-19q, 1q+, monosomy 8trisomy 15 and 20 (18.9%)
III (n=14)**	7 (50%)	4 (28.5%)	19p+, trisomy 5 and 20, 9q-,17q- (21.4%)

* 3 cases had some but not all features of grade II, **2 cases had non-meningothelial tumors in differential.

Conclusions: The integration of histopathology with complex genetic/genomic data, results in the improved identification of clinically distinct meningioma subgroups, which in turn directs the clinical care plan for certain patients. Such results will also facilitate the development of targeted therapeutic strategies.

1776 The Genomic Copy Number Profile of Angiomatous Meningioma

MS Abedalthagafi, SH Ramkissoon, KL Ligon, AH Ligon, RD Folkerth, S Santagata. Brigham and Women's Hospital and Harvard Medical School, Boston, MA.

Background: Angiomatous meningioma is an uncommon World Health Organization (WHO) grade I subtype of meningioma. It has numerous small or large vascular channels which may predominate over the meningothelial elements, often making the diagnosis challenging. We present here novel genomic copy number signatures of three cases of angiomatous meningioma.

Design: We studied three cases of angiomatous meningioma (from two females and one male). The mean age of the patients is 75 years. Array-based comparative genomic hybridization (aCGH) was performed using the stock 1x1M Agilent SurePrint G3 Human CGH Microarray chip to identify tumor-specific genomic copy number changes in FFPE clinical samples (Craig JM., et al., PLoS One. 2012; 7(6):e38881).

Results: aCGH revealed polysomy (i.e., more than two copies) of several chromosomes including: 5, 6, 7, 12, 13, 15, 16, 17, 18, 19, 20, 21, and 22. Interestingly, the common genomic variants in type I meningioma, like monosomy 22 or 1p loss or neutral copy number changes, were not observed in angiomatous meningioma.

Conclusions: Angiomatous meningiomas generally share histologic, prognostic and clinical features of other WHO grade I meningiomas. Data from our three cases suggests that this meningioma subtype might have a unique genomic copy number profile. Because the angiomatous subtype can sometimes pose diagnostic difficulty to pathologists due to confusion with other vascular meningeal lesions the presence of chromosomal trisomies might be of significant diagnostic utility. Moreover, our findings might help elucidate the pathogenesis of these tumors. Evaluation of additional tumors of this subtype is now needed.

1777 High Expression of Olig2 Is Restricted to Gliomas and Is More Common in Oligodendrogliomas Than Astrocytomas

CL Appin, C Cohen. Emory University School of Medicine, Atlanta, GA.

Background: Olig2, a bHLH transcription factor, is restricted to oligodendroglial differentiation in normal human brain, but has been found to be expressed in both oligodendrogliomas and astrocytomas of different grades. As such, this marker is not useful in differentiating an oligodendroglioma from an astrocytoma but is used to distinguish a glioma from other central nervous system (CNS) and non-CNS malignancies. Results from studies assessing Olig2 expression are mixed, with some finding stronger expression in oligodendrogliomas compared to astrocytomas while others show equal expression in the two groups. Additionally, Olig2 expression has been found in other CNS as well as non-CNS tumors. The purpose of this study was to assess Olig2 expression in oligodendrogliomas, astrocytomas and various non-CNS tumors.

Design: Tissue microarrays (TMAs) of glioblastoma (GBM) tumors (n=27) and anaplastic astrocytomas (n=21) as well as individual cases of oligodendrogliomas (n=20) were assessed for Olig2 expression. A TMA of non-CNS tissue (both malignant and normal), including tonsil, breast, placenta, prostate, colon, thyroid, skin, pancreas, ovary, mesothelium, testis, thymus, liver, spleen, and salivary gland, was also stained for Olig2. Also included were cerebral cortex and pituitary gland (one case each). Each tumor was assigned an intensity (1+ to 3+) and the percentage of cells staining was determined. The intensity and percentage of cells staining for each tumor was multiplied to give a q-score (0 to 300). Statistical analysis was performed using the Wilcoxon rank-sum test.

Results: Oligodendrogliomas showed significantly higher expression of Olig2 compared to other gliomas combined ($p < 0.001$). Gliomas as a whole likewise showed significantly higher Olig2 expression compared to non-CNS tumors ($p < 0.001$). Intensity of staining in gliomas ranged from 0-3+ while that of non-CNS tumors ranged from 0-1+.

Conclusions: High expression of Olig2 is seen only in gliomas, although faint immunoreactivity is present in some non-CNS tumors. Oligodendrogliomas show stronger immunoreactivity compared to astrocytomas.

1778 Meningiomas That Meet Grade II by 3 Criteria Have an Increased Rate of Recurrence

CL Appin, SG Neill, RH Press, RS Prabhu, I Crocker, DJ Brat. Emory University School of Medicine, Atlanta, GA.

Background: Meningiomas are graded according to the World Health Organization (WHO) criteria as grade I, II or III. While grade I meningiomas are considered benign, grade II and III tumors recur more frequently and have a worse prognosis. Criteria for classification as grade II include 1) brain invasion; 2) specific histologic patterns (chordoid and clear cell); 3) increased mitoses; and 4) the presence of at least 3 of 5 atypical features (increased cellularity, sheet-like growth, prominent nucleoli, 'spontaneous' or 'geographic' necrosis and small cells with a high nuclear to cytoplasmic ratio). The purpose of this study was to determine whether meningiomas that meet more than one criterion for grade II are more aggressive than those that meet only one criterion.

Design: Seventy-one grade II meningiomas resected at Emory University Hospitals from 2000-2010 were included. Slides, pathology reports, and patient charts from each case were reviewed. Meningiomas were grouped according to number of histopathologic criteria met to establish a grade II diagnosis and correlated with time to recurrence and survival data. Median follow-up time was 3.2 years. Statistical analysis was performed using Fisher's exact test and SAS-JMP software.

Results: Meningiomas that met 3 criteria (n=7) for classification as a grade II neoplasm had a higher recurrence rate (85.7%) than those that only met one (n=39) or two (n=23) criteria (33.3%; p=0.0146 and 26.1%; p=0.0086, respectively). No significant difference

in recurrence rates were noted for meningiomas that met one criterion compared to those that met two. Within the timeframe of follow-up, time to recurrence and patient survival did not differ between study groups.
Conclusions: Meningiomas that meet 3 criteria for grade II have a higher recurrence rate than those that meet 1 or 2 criteria.

1779 Post-Surgical Outcome for Epilepsy Associated with Type I Focal Cortical Dysplasia Subtypes

SL Barclay, RA Prayson. Cleveland Clinic Lerner College of Medicine, Cleveland, OH; Cleveland Clinic, Cleveland, OH.
Background: Focal cortical dysplasias (FCDs) are a well-recognized cause of medically intractable seizures. There have been numerous published attempts at classification schemes, indicative of disagreement in definition and approach. The clinical relevance of certain subgroups of the ILAE classification scheme, including subtypes of FCD type I remains to be determined. The aim of the present work is to assess the effect of histologic subtype of FCD I, specifically types Ib and Ic, on surgical outcome with respect to seizure frequency for patients with medically intractable epilepsy. This study also provides an opportunity to compare the predictive value of the ILAE and Palmini et al. classification schemes with regard to the type I FCDs and seizure outcome.
Design: We retrospectively reviewed 91 patients [54.9% female; median age: 19 years (interquartile range 8-34 years); median seizure duration: 108 months (interquartile range 36-204 months)] with medically intractable epilepsy who underwent surgery and who were diagnosed with FCD. We compared the pathological subtypes, evaluating the patients' post-surgical outcome with respect to seizure frequency according to Engel's classification or according to the ILAE outcome classification. Both the ILAE classification scheme and Palmini et al. pathologic classification scheme were utilized. We calculated the crude outcome analyses with a chi-square and a Fisher's exact test.
Results: Of the 91 patients, there were 50 patients with ILAE FCD type Ib, 41 with ILAE FCD type Ic, 63 with Palmini et al. FCD type IA, and 28 with Palmini et al. FCD type IB. After surgery, 44 patients (48.4%) became completely seizure free. Crude analysis revealed no significant difference between patients with subtypes of ILAE FCD type I or Palmini et al. FCD type I concerning postoperative outcome according to the Engel and ILAE scoring systems on seizure frequency.
Conclusions: Our findings revealed no significant difference concerning surgical outcome with respect to seizure frequency for the histologic subtypes of ILAE FCD type I (Ib vs. Ic) or Palmini et al. FCD type I (IA vs. IB). In isolation, the histologic subtype of FCD type I does not appear predictive of postoperative outcome.

1780 Outcomes of Subtype-Specific Mutations and Gene Expression in Medulloblastoma

GA Bien-Willner, R Mitra. Washington University, St. Louis, MO.
Background: Medulloblastoma (MB) is the most common malignant pediatric brain tumor. Although the 5-year overall survival for patients is ~80%, current standard treatment includes cranial and axial irradiation that results in significant morbidity and mortality. Thus, is it paramount to identify patients who may benefit from more or less treatment *a priori*, and to this end molecular markers are being developed to predict outcomes for standard and high-risk patients. Current studies have identified four basic subtypes of MB: those with aberrant WNT or SHH signaling, as well as the under-characterized groups "C" and "D". Little is known about group D other than it commonly harbors the most frequently observed chromosomal abnormality in MB, i17q, whose presence confers a higher risk of recurrence in standard-risk patients. Recent publications have identified mutations that are specific or overrepresented to this group. Among these are mutations in genes related to DNA methylation, which may underlie the oncogenic process. We sought to validate the specificity of these mutations in our cohort of 57 MB samples; to assess if the mutated genes were expressed differently across the different MB subtypes and possibly contribute to the disease process; and to identify any prognostic value to these mutations.
Design: DNA was extracted from 57 FFPE MB cases. A microfluidics-based approach (Fluidigm) was used to amplify all exons of six group D specific genes: *KDM6A, ZMYM3, MLL3, GPS2, THUMPD3*, and *CTDNEP1*. The resulting amplicons were sequenced with the MiSeq 2x 250 platform. Expression data for 103 MB cases was extracted from available archives. Statistical comparisons between different MB subtypes were undertaken with the R statistical package. R was also utilized for survival (Kaplan-Meier) analysis.
Results: Gene sequencing uncovered coding mutations in *MLL3, THUMPD3*, and *KDM6A,* and *CTDNEP1*. These mutations were not specific to i17q in our cohort. KDM6A is expressed at significantly higher levels in females compared to male patients, and is seen in lower levels in Groups C /D compared to SHH and WNT, particularly in the presence of i17q. GPS2 and CTDNEP1 expression was also correlated negatively with i17q. ZMYM3 was lowest in SHH patients, while MLL3 expression was highest in groups C and D, particularly in the absence of i17q.
Conclusions: Although patients with identified mutations tended to relapse and die, there was not enough statistical power in our cohort to draw conclusions. Differences in gene expression may help stratify patients based on molecular subtype, but further studies are warranted.

1781 Whole Genome SNP Array Analysis of Ependymoma and Anaplastic Ependymoma

C Cai, V Hucthagowder, DH Gutmann, S Kulkarni, S Dahiya. Washington University School of Medicine, St. Louis, MO.
Background: Ependymomas account for ~3-9% of all neuroepithelial tumors in adults. In children under 3 years of age, these tumors represent ~30% of nervous system neoplasms. Although these grade II tumors can undergo anaplastic changes (grade III tumor), current diagnostic criteria are subjective and not clearly defined in the WHO grading system. In an effort to develop molecular criteria for a more accurate subclassification of ependymoma, we sought to identify specific genomic alterations that correlate with tumor type and/or grade using high resolution SNP arrays.
Design: We identified 5 ependymomas (WHO grade II), 1 anaplastic ependymoma (WHO grade III) and 2 ependymomas with focal anaplasia (WHO grade III) from in-house surgical cases with available histological slides and sufficient formalin-fixed, paraffin-embedded (FFPE) tissue. The ependymal lining of the floor of 4th ventricle from normal, age-matched autopsy brains was used as normal controls (n=2). Whole genome SNP array using Affymetrix CytoScan HD assay was performed followed by analysis of array data using Affymetrix Chromosome Analysis Suite v2.0. Additional bio-informatics analysis was performed using Biodiscovery Nexus v7 and Partek genomics suite software.
Results: All tumors, regardless of malignancy grade, harbored 5p15.31 gain. In addition, the grade III ependymomas (including ones with focal as well as overt anaplasia) had chromosomal losses on 9p21, 14q21 and 18p11.32.
Conclusions: Consistent gain of 5p15.31 in ependymoma may represent a potential diagnostic marker. Although this series contains a limited number of cases, consistent losses of chromosomes 9p21, 14q21 and 18p11.32 suggests that genes in these loci may facilitate malignancy progression.

1782 Neuropathology of Middle Aged Subjects with Homozygous ApoE4 Genotype (Preclinical Alzheimer's Disease) Indicates Spatial and Temporal Disconnect between Amyloid-beta and Phospho-Tau

RJ Castellani, KT White, A Fashori, BX Li, R Johnson, HR Zielke. University of Maryland, Baltimore, Baltimore, MD.
Background: The failure of lesion-directed therapies for Alzheimer's disease (AD) has led to the suggestion that fully developed AD, even if clinically moderate, is too advanced to benefit from lesion removal. This has raised interest in studying early as well as preclinical disease, and emphasizes the need to better characterize brain tissue from middle aged subjects.
Design: Genomic DNA from frozen brain tissue from 269 consecutive subjects (ages 30 -60). Each case was characterized for Apolipoprotein E (APOE) genotype, by far the strongest genetic risk factor for sporadic AD. PCR and restriction enzyme analysis was used according to standard methodology. The allelic frequencies (E2, E3, and E4) were consistent with a population from the Northeastern US. Nine of the 254 cases were homozygous APOE4. We then sampled all Brodmann areas from the cerebral cortex and lower neuraxisfrom all homozygous APOE4 cases, as well as three E2/E2, five E2/E3, five E3/E3, and five E3/E4 subjects. Antibodies to phosphorylated tau and amyloid-beta (monoclonal antibodies AT8 and 4G8, respectively) were applied immunohistochemically to all brain sections in all cases.
Results: The most remarkable finding was that significant diffuse amyloid-beta deposits, as well as neuritic plaques, were present in all of the homozygous APOE4 cases, as young as age 34. Consistent amyloid-beta deposits were present in all heterozygous E3/E4 subjects, and essentially no amyloid beta deposits were present in other genotypes. Phospho-tau immunoreactivity, however, was variable across subjects regardless of genotype. Some subjects in their late 50's had little AT8 reactivity (Braak Stage I-II), while one subject had Braak stage V AT8 reactivity. Moreover, AT8 reactivity was showed no spatial relationship with 4G8 reactivity.
Conclusions: This study confirms that E4 predisposes to amyloid-beta pathology in a co-dominant fashion, but also indicates that insoluble tau deposits are variable and more closely aligned with aging per than AD risk, indicating amyloid-beta and tau deposits in middle age occur by independent mechanisms, contrary to the widely accepted amyloid cascade hypothesis. In addition, there was no evidence of "spreading tauopathy" as a function of AD risk.

1783 Recurrent Grade I Meningiomas

A Celebre, MY Wu, DG Yarlett, M Cusimano, D Sunit, JR Karamchandani. University of Toronto, Toronto, ON, Canada.
Background: Recurrence rates for WHO grade I meningioma at 5, 10, and 15 years are 18%, 26%, and 32%. Identifying markers to better predict risk of recurrence(ROR) in grade I meningiomas offers the potential to inform treatment decisions with regards to adjuvent radiotherapy.
Design: We analyzed NCBI dataset GSE16181 along with a literature review to identify candidate markers for increased ROR. We built a TMA including 149 specimens including 51 recurring(rMening) and 98 non-recurring(nrMening) tumors. Immunohistochemistry(IHC) was performed for the following proteins: Hephaestin(Heph), chloride intracellular channel 1(Clic1), p63, and Ki67, as well as 4 markers of epithelial-mesenchymal transition(EMT): E-Cadherin(ECad), N-Cadherin(NCad), Slug, and Snail. Protein expression was quantified with digital image analysis.
Results: GSE16181 was analyzed with GenePattern. Logistic regression analysis identified 60 genes that best classified rMening and nrMening. 40 genes were common to both analyses. Mean IHC expres. of rMening and nrMening:

Table 1: Quantitative protein expression

	N		Mean Protein Expression		
Protein	rMening	nrMening	rMening	nrMening	p=
Heph	51	92	88.88	76.60	<.001*
Clic1	51	95	90.33	84.27	.01*
ECad	51	95	48.73	49.53	.80
NCad	51	81	78.68	88.00	.001*
Snail	51	97	28.77	49.01	<.001*
Slug	51	98	73.91	87.87	<.001*
p63	51	97	16.15	12.99	.04*
Ki67	50	98	4.49	3.97	.017*

* p<.05

Expres. of p63 and Ki67 was significantly higher in rMening. Data comparing first occurrences and paired recurrences:

Table 2

		Mean Protein Expression		
Protein	N	1st Occurence	1st Recurrence	p=
Heph	22	83.5	91.49	.104
Clic1	21	85.32	94.26	.021*
ECad	22	46.03	49.00	.631
NCad	22	78.73	80.85	.726
Snail	22	22.70	37.07	>.001*
Slug	22	69.31	80.41	.058
p63	22	15.09	18.87	.010
Ki67	22	4.33	4.58	.486

* p<.05

Conclusions: Snail and Slug generally showed higher expression in recurrent tumors, potentially implicating activation of EMT pathways in recurrence.

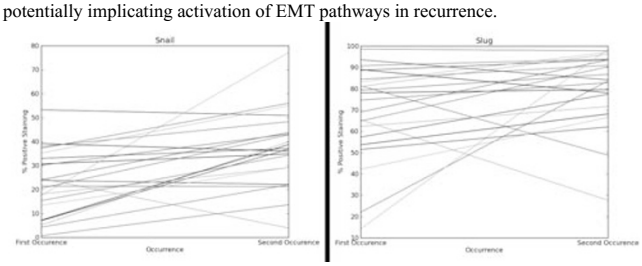

Ki67, p63, and Clic1 showed significantly different protein expression in rMening and nrMening, but overlapping expression profiles precludes IHC-based classification.

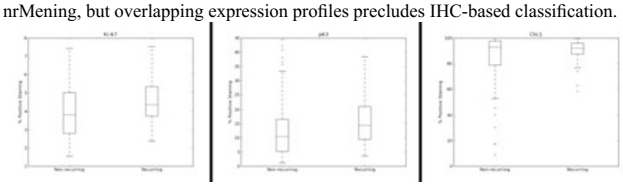

1784 Immunohistochemical Examination of Adipophilin Expression in Hemangioblastomas

JC Chang, EJ Cochran. Medical College of Wisconsin, Milwaukee, WI.

Background: Hemangioblastomas (HB) are uncommon tumors of the central nervous system (CNS), accounting for 2.5% of all intracranial tumors. Histologically, these tumors are characterized by an intimate mixture of endothelial cells, pericytes, and vacuolated stromal cells, the cytoplasm of which contains lipid vacuoles and can be highlighted with Oil Red O on frozen sections. Recently, adipophilin has been shown to be a useful immunohistochemical (IHC) marker for cells containing intracytoplasmic lipid droplets, usually in the context of cutaneous sebaceous neoplasms. Herein, we investigate the expression of adipophilin in a large series of HB and other CNS tumors to assess its utility as a diagnostic marker.

Design: IHC staining for adipophilin was performed on 27 cases of HB and 17 other intracranial tumors. IHC was performed on whole-section slides following antigen retrieval using a polyclonal rabbit antibody to adipophilin, and the staining pattern was semi-quantitatively assessed. The extent of immunoreactivity was graded according to the percentage of positive tumor cells.

Results: All 27 (100%) cases of HB showed immunoreactivity for adipophilin with 24/27 (89%) cases showing strong, diffuse positivity. One case showed patchy positivity in 50% of tumor cells, and two cases showed scattered positivity in 10-20% of cells. By comparison, adipophilin was negative in all cases of pilocytic astrocytoma (2), diffuse astrocytoma (2), pleomorphic xanthoastrocytoma (2), clear cell meningioma (1), secretory meningioma (1), myxopapillary ependymoma (1), ependymoma (1), and chordoma (1). Only metastatic renal cell carcinomas (3 of 3) and a single case of lipidized glioblastoma multiforme (1 of 3) showed a staining pattern similar to HB.

Conclusions: Our data demonstrate that adipophilin is a sensitive marker for hemangioblastomas, and has the additional advantage over Oil red O that it can be performed on formalin-fixed paraffin-embedded tissue. However, other immunostains must be employed to rule out a metastatic renal cell carcinoma, particularly in the setting of von-Hippel Lindau syndrome.

1785 Evaluation of Simultaneous Muscle and Nerve Biopsies for Diagnosis

DJ Chen, RA Prayson. Cleveland Clinic, Cleveland, OH; Cleveland Clinic Lerner College of Medicine, Cleveland, OH.

Background: Skeletal muscle and peripheral nerve are occasionally simultaneously biopsied with the goal of increasing diagnostic yield in patients with an uncertain clinical diagnosis or in cases where the pathology is known to be focal or multifocal (e.g. vasculitis or amyloidosis). The purpose of the present study is to evaluate the diagnostic utility of performing simultaneous muscle and nerve biopsies.

Design: A surgical pathology database was searched from 1993 to 2011 to identify patients who had concomitant skeletal muscle and peripheral nerve biopsies. Demographic (age, gender, and biopsy site) and pathologic (histologic and electron microscopic) findings were recorded for all cases.

Results: Two-hundred and eighty-seven patients were included for study. There were 161 (56.1%) males and 126 (43.9%) females with a mean age at time of biopsy of 50.8 years. The most commonly sampled sites were gastrocnemius muscle (n=186, 64.8%) and sural nerve (n=264, 92%). The majority of cases (n=226, 78.7%) were found to have a definitive diagnosis in either muscle or nerve. Of the cases with definitive diagnoses, 53 (23.4%) were based off the muscle only, 127 (56.2%) off the nerve only, and 46 (20.4%) had a definitive diagnosis in both the muscle and nerve. The most common diagnoses made on muscle biopsy alone were denervation atrophy (n=32) and type II muscle fiber atrophy (n=12). The most common diagnosis made on nerve biopsy alone was a mild or greater degree of axonal loss (n=112). Vasculitis was found in muscle-only in 5 cases, nerve-only in 14 cases, and both muscle and nerve in 4 cases. Amyloidosis was exclusive to muscle in no cases, was seen in nerve-only in 1 case, and was found in both muscle and nerve in 4 cases.

Conclusions: Performing simultaneous muscle and nerve biopsies can improve diagnostic yield. For patients who had a diagnosis following concomitant biopsies, the yield increased from 16% to 78.7%. Of the 28 patients with either vasculitis or amyloidosis, up to 20 may have gone undiagnosed if simultaneous biopsies had not been performed.

1786 Identification of Viral Pathogens by Unmapped Next Generation Sequencing Reads in Glioblastoma

PJ Cimino, G Zhao, W David, EJ Duncavage. Washington University School of Medicine, St. Louis, MO.

Background: Viral pathogens have been implicated in the development of many cancers including human papillomavirus (HPV) in squamous cell carcinoma and Epstein-Barr virus (EBV) in Burkitt's lymphoma. However, the significance of viral pathogens in brain tumors is controversial, and cytomegalovirus (CMV) has been associated with glioblastoma (GBM) in some studies; the role of CMV in GBMs, if any, is unclear. In this study we sought to determine if viral pathogen sequences could be discovered in an unbiased manner from unmapped next-generation sequencing (NGS) reads obtained from targeted oncology, panel-based sequencing of GBMs.

Design: We identified 21 sequential GBM cases that were analyzed by a targeted NGS clinical oncology panel containing 151 genes using DNA obtained from formalin-fixed paraffin-embedded GBM tissue. Sequencing reads that did not map to the human genome were first filtered and low quality reads removed. High quality reads were then extracted and sequentially aligned to the NCBI nt database using blastn and NCBI nr protein database using blastx. Aligned reads were classified based on NCBI taxonomy database and all eukaryotic viral sequences were further classified into viral families. Subsequent confirmatory *in-situ* hybridization (ISH) was performed for EBV on cases for which sufficient remaining material existed.

Results: Of the 21 GBM cases an average of 38,000 non-human reads (1.9%) did not align to the human genome and were used for viral sequence identification. The two most highly recurrent viral sequences (both herpesviruses), Epstein-Barr virus (EBV) and Roseolovirus were detected in 5/21 (23.8%) cases and in 1/21 (4.8%) cases, respectively. The presence of EBV and Roseolovirus were mutually exclusive. None of the cases had detectable CMV. Of the 5 GBM cases with detectable EBV DNA, only one had additional material for EBV ISH. This case did not demonstrate detectable EBV RNA.

Conclusions: Using an unbiased approach based on analysis of off-target, non-human NGS reads coupled with a novel viral discovery pipeline, we discovered that a subset of our GBM cases harbor detectable EBV DNA, however it is unclear if EBV is actually expressed or represents latent viral infection in lymphocytes that cross the disrupted blood brain barrier which accompanies many GBMs. A similar approach using off-target non-human NGS reads could be used to discover viral sequences in other cancer types in which targeted NGS has been performed.

1787 Specificity of Immunohistochemical Markers of Differentiation in the Sellar Region: Implications for the Diagnosis of Metastatic Carcinoma

MD Cykowski, SZ Powell, H Takei, DS Baskin, AL Rivera. Houston Methodist Hospital, Houston, TX.

Background: Sellar region metastases have been documented for lung, breast, kidney, liver, and gastrointestinal tract carcinomas, among other sites. Metastases may be considered in patients with history of carcinoma, in cases with radiologic features atypical for adenoma, or in cases with histologic features discordant with radiology suggestive of adenoma. Immunohistochemical (IHC) panels may be pursued in each of these situations, more so if histologic features are equivocal. However, there is limited data regarding the specificity of IHC markers of differentiation in contemporary surgical pathology practice when these are applied in the sellar region.

Design: Pituitary adenoma diagnoses made at our institution in the last 8 years were reviewed. Tumors selected for study included a variety of functional and non-functional adenoma subtypes. Histologic features were reviewed and unstained sections were submitted for IHC studies with cytokeratin 7 (CK7), cytokeratin 20 (CK20), gross cystic disease fluid protein-15 (GCDFP-15), estrogen receptor (ER), Napsin A, thyroid transcription factor-1 (TTF-1), PAX-8, and Hep Par1. IHC stain results were compared to controls and graded as negative (score 0), weakly positive/equivocal (score 1), moderately positive (score 2), and strongly positive (score 3), and specificity was calculated.

Results: Twenty-four tumors studied (11 females; mean age of 52.5 years) included 7 corticotrophic, 5 gonadotrophic, 3 somatotrophic, 2 lactotrophic, 3 null cell, and 4 plurihormonal adenomas. Mean tumor size was 2.9 cm. Specificity was 100% for GCDFP-15, TTF-1, and CK20. Specificity was 96% for PAX-8 and Hep Par1 with both strongly staining (focally) a plurihormonal growth hormone secreting adenoma in a patient with acromegaly. The remaining test specificities were 46% (IHC score>0) and 75% (score>1) for Napsin A, 75% (IHC score>0) and 79% (score>1) for ER, and 52% for CK7.

Conclusions: CK7 demonstrated strong, scattered positivity in 11 tumors and 6 of these demonstrated weak/equivocal or positive Napsin A staining. Napsin A stain highlighted cytoplasmic granules in most positive cases. CK7 was also positive in 4 of 6 ER-positive tumors. Therefore, GCDFP-15 and TTF-1, both demonstrating 100% specificity, are most informative in the setting of presumed breast and lung metastases to the sella, respectively. Conversely, positive IHC results with standard pituitary hormone markers (e.g., growth hormone) are likely to be spurious in the setting of a sellar tumor with GCDFP-15, TTF-1, PAX-8, Hep Par1, or CK20 positivity.

1788 Molecular Profile of a Cohort of 219 Low-Grade Gliomas

G De Maglio, T Ius, G Falconieri, F Marchesin, E Masiero, S Cernic, M Skrap, S Pizzolitto. University Hospital, Udine, Italy.

Background: Low-Grade Gliomas (LGG) are heterogeneous neoplasms characterized by a slow growth rate, tendency to anaplastic transformation and variable clinical behavior. Several studies suggest a prognostic stratification of LGG patients according to histological classification and molecular markers, yet the prognostic and predictive role of molecular profiling in LGG is controversial.

Design: A series of 183 WHO II LGG and 36 WHO II-III gliomas consecutively resected between 2000-2013 was molecularly investigated: 1p/19q deletion status was assessed by means of FISH. Quantitative MGMT methylation and IDH1-2 status were performed by pyrosequencing, and p53 immunostaining was done as well. A microscopic reappraise was preliminarly carried out according to the 2007 WHO Classification of brain tumors.

Results: Histological classification and molecular profiles are summarized in table1.

		1p/19q	MGMT	IDH1-2	p53
Oligodendroglioma	n=21	88.2%	90%	85.7%	10%
WHO II (n=18)		86.7%	88.2%	83.3%	5.9%
WHO II-III (n=3)		100%	100%	100%	33.3%
Astrocytoma	n=128	7.9%	88.8%	80.3%	77.3%
WHO II (n=106)		8.2%	91.7%	82.9%	78.3%
WHO II-III (n=22)		4.5%	75%	68.2%	72.7%
Oligoastrocytoma	n=70	64.1%	98.6%	92.9%	57.1%
WHO II (n=59)		64.2%	98.3%	91.5%	61%
WHO II-III (n=11)		63.6%	100%	100%	36.4%

Among IDH mutated cases, rather than IDH1-R132H, we documented unusual mutations including IDH1-R132C (n=6), IDH1-R132G (n=3), IDH1-R132S (n=2), IDH2-R172K (n=4), IDH2-R172S (n=1). We subdivided patients in methylation classes according to the median percentage of methylation revealed among the 10 CpG islands analyzed, and we observed an increased rate of IDH mutation from unmethylated (medium methylation <9%) to highly methylated tumors.

	IDH mut
unmethylated (n=25)	36%
methylation 9-20% (n=67)	86.6%
methylation 20-40% (n=72)	91.7%
methylation 40-60% (n=24)	95.8%
methylation >60% (n=9)	100%

All cases (n=62) with 1p/19q deletion had also MGMT methylation and IDH1-R132H mutation (n=60) or IDH2-R172K mutation (n=2).

Conclusions: To the best of our knowledge, this study is one of the larger record of LGG primarily resected at a single institution. Our results indicate that there is a highly significant (chi-square test, P=0.000*)* association of 1p/19q codeletion with IDH mutation, MGMT methylation and p53, and between MGMT methylation and IDH mutation.

1789 Next-Generation Sequencing of Cancer Gene Panel in Glioblastoma Reveals Intriguing Findings

CJ Ferguson, DH Gutmann, JD Pfeifer, S Dahiya. Washington University, Saint Louis, MO.

Background: BRAF mutation and rearrangement are common in low-grade CNS tumors. However, the frequency of these events is much lower in glioblastoma (GBM). The purpose of this study was to determine whether BRAF mutations are found in GBM from specific brain locations.

Design: A major effort in the modern approach to treating malignancy is the identification of patient-specific driver mutations for targeting with specific therapeutics. Our institution has developed a clinical test that uses massive parallel sequencing of a panel of 41 cancer genes to identify actionable mutations. We analyzed 25 cases of GBMs from this database for the predicted pathogenic (level 1) mutations.

Results: All but one sequenced GBM were supratentorial, with the most common site being the frontal lobe (9 cases), followed by parietal lobe (6 cases), temporal lobe (4 cases), periventricular region (3 cases), occipital lobe (2 cases), and thalamus (1 case). All three of the periventricular cases harbored pathogenic missense mutations within the BRAF kinase domain, 2 of which were previously unreported. Furthermore, these three cases were negative for EGFR mutation and/or amplification (confirmed by fluorescence *in situ* hybridization analysis). These findings are in contrast to the GBM tumors arising in other locations, which all lacked *BRAF* mutation but harbored EGFR mutations and/or amplifications (~36% cases). There was also a statistically significant difference in the age of the two groups, with *BRAF* mutations found in younger patients (p value = 0.0042).

Conclusions: These findings suggest that GBM arising in the periventricular location is more likely to harbor *BRAF* mutations and tends to occur in younger individuals. In addition, the absence of *EGFR* mutation in these tumors raises the intriguing possibility that these molecular events are mutually exclusive. These observations support the notion that GBM tumors harbor spatial and temporal 'genetic' heterogeneity.

1790 Presence and Maintenance of BRAF V600E Mutation in a Pilocytic Astrocytoma Evolving into a Ganglioglioma

PO Fiset, AM Fontebasso, N Jabado, S Albrecht. McGill University Health Center, Montreal, QC, Canada.

Background: Gangliogliomas (GGs) are tumours of, unclear histogenesis, which consist of dysplastic neurons and variable amounts of a glial component. We present a case of a 4 year old patient with a right cerebellar hemispheric tumor, which was resected in two stages in 2006 and 2007 and recurred in 2011 and 2013. The first 3 specimens were histologically compatible with a pilocytic astrocytoma (PA). However, the 4th specimen contained a combination of many dysplastic neurons with a glial component, consistent with a GG.

Design: Immunohistochemistry for neuronal and glial proteins was performed on all specimens. DNA was extracted from formalin-fixed paraffin embedded and frozen tissue. DNA was analyzed by BRAF V600E high resolution melting (HRM) analysis.

Results: The possibility of the primary tumour being a GG masked by an exuberant glial component cannot be completely excluded; however, all specimens had been submitted in toto, and the primary tumour and first recurrence did not show any dysplastic neurons. By immunohistochemistry, cells from the initial PA resections showed GFAP and MAP-2 positivity and SMI-32 negativity. The last recurrence of GG showed numerous dysplastic ganglion cells strongly positive for MAP-2 and SMI-32, but negative for NeuN; GFAP positivity was restricted to the glial component. HRM analysis indicated a BRAF V600E mutation in all specimens. Furthermore, HRM analysis demonstrated a unique profile for the GG, suggesting potentially novel alterations in the BRAF sequence.

Conclusions: This is an unusual case of a cerebellar PA, which appears to have evolved into a GG. This may highlight a potential pathway for histogenesis of GGs and point to a role of the BRAF V600E mutation as the oncogenic driver. More data obtained through next-generation sequencing of this entity and comparison with other PAs and GGs with BRAF V600E mutations may elucidate the molecular pathogenensis for both these tumours.

1791 Can Nogo-A and Alpha-Internexin Immunohistochemical Markers Distinguish Prognostically Distinct Oligodendro-Gliomas and Astrocytomas?

D Gertsch, S Sharma. Georgia Regents University, Augusta, GA.

Background: Gliomas, the most common primary brain tumors, are histopathologically classified primarily into prognostically distinct diffuse astrocytomas or oligodendrogliomas. However, with the exception of 1p19q codeletion in oligodendrogliomas, no other markers reliably differentiate these gliomas. We evaluated the differences in expression of Nogo-A and alpha-internexin (INA) between astrocytomas and oligodendrogliomas, and between gemistocytes (often high-grade astrocytic) and mini-gemistocytes (oligodendroglial).

Design: Fifty archival cases of oligodendrogliomas (13) and astrocytomas (37) of all histologic grades were immunostained for alpha internexin and Nogo-A, with autopsy cerebral and cerebellar tissue as positive control. The staining of tumor cells were interpreted as 1+ (<10% positive cells), 2+ (11-50%) and 3+ (>50%), while carefully excluding the known immunostaining of native neurons and axons.

Results: Extensive (3+) staining with Nogo was seen in 5/13 (38%) oligodendrogliomas, 2/14 (4%) anaplastic astrocytomas (AA-3) and 1/23 (14%) glioblastoma (GBM) (overall 3/37, 8% astrocytomas). Extensive (3+) staining with INA was seen in 5/13 (38%) oligodendrogliomas but in 0/37 (0%) astrocytomas. While some staining with INA was seen in 7/7 (100%) oligodendrogliomas with 1p19q codeletion and in 2/3 (66%) without the codeletion, however >10% cell staining was seen in only 4/7 (57%) oligodendrogliomas with codeletion (comparable to Buckley et al). Minigemistocytes were stained in 11/11 (100%) oligodendrogliomas with Nogo and in 11/12 (82%) with INA. In contrast, gemistocytes were stained in only 1/35 (3%) astrocytomas with Nogo, but none stained with INA.

Conclusions: Our study showed extensive immunoexpression (>50% tumor cells) of Nogo-A or alpha-internexin in 38% oligodendrogliomas (more selective than the literature), but only 8% and 0% in astrocytomas, respectively. Furthermore, high expression of Nogo and INA in oligodendroglial mini-gemistocytes in contrast to rare expression with Nogo in gemistocytes and none with INA, may be of diagnostic and favorable prognostic value.

1792 Severe Congenital Hydrocephalus and Systemic Lymphangiogenesis in Double Knockout Mice for Anti-Angiogenic Proteins, Thrombospondin-1 (TSP-1) & Pigment Epithelium-Derived Factor (PEDF)

MA Guzman, SM Habeebu, PS Fitchev, ML Cornwell, SE Crawford. Saint Louis University, Saint Louis, MO.

Background: Thrombospondin-1(TSP-1) and Pigment Epithelium-derived Factor (PEDF) are two of the most potent endogenous inhibitors of angiogenesis and have neurotrophic activity. PEDF also acts as a neuronal survival factor. Ablation of TSP-1 or PEDF in mice promotes increased angiogenesis; however very limited studies have explored their role in brain development and lymphatic vessels.

Design: TSP-1 knockout (KO) mice were crossed with PEDF null mice on a C57Bl6 background and the double knockouts (n=18) were confirmed by genotyping. Age-matched wild type (WT) controls (n= 16) were evaluated. Phenotypic characterization

was performed on 1 mo (n = 6), 3 mo (n=6), and one year (n=6) by gross and histological examinations. Tissue sections were immunostained with Factor VIII, VEGF, VEGF-C . Microvascular density (MVD) was assessed in five non-overlapping hpf in each group.
Results: Severe hydrocephalus was observed in 28% of the double KO animals.

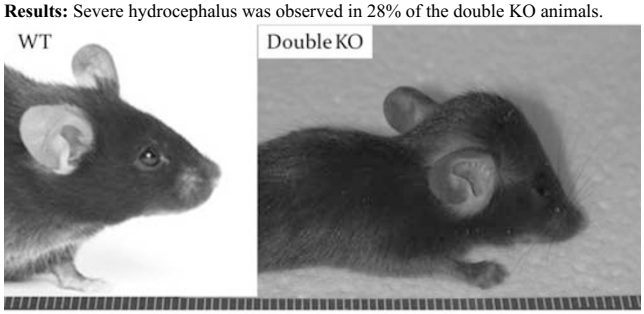

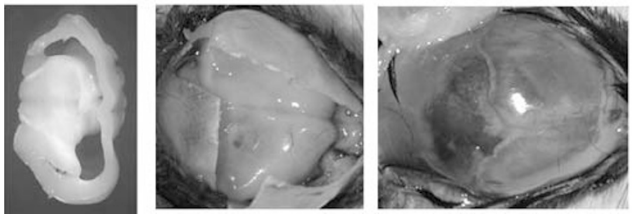

Ependimal cells of the subcomissural organ (SCO) demonstrated abnormally fused cilia.

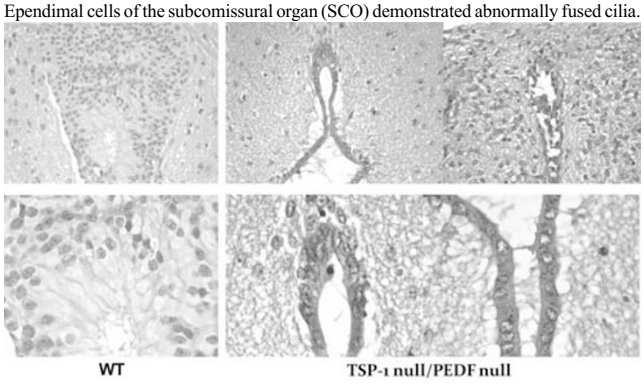

Tufts of angiomatous vessels were also seen in the leptomeninges. The double knockout had a nearly 5 fold increase in angiogenesis and red cell extravasation was evident suggesting increased vascular permeability. A lymphatic malformation adjacent to the pancreas caused cyst formation in 22% of the KO mice. TSP-1 and PEDF proteins were expressed in lymphatics of the WT mice.
Conclusions: Concurrent loss of TSP-1 and PEDF causes severe hydrocephalus, abnormal fusion of ependymal cilia in the SCO and tufts of angiomatous vessels in the leptomeninges. Systemic vasculopathy involving both capillaries and lymphatic vessels was observed. In a subset of mice, a cyst-like lymphatic malformation invaded the pancreatic region. In summary, this new mouse model highlights the importance of TSP-1 and PEDF in regulating normal brain and vascular development.

1793 Integrated Genomic and Transcriptomic Analysis of Glioblastoma with Oligodendroglioma Component

BH Hinrichs, S Newman, MR Rossi, DJ Brat. Emory University School of Medicine, Atlanta, GA.

Background: Glioblastoma with oligodendroglioma component (GBM-O) is a recently recognized subtype of GBM demonstrating both astrocytic and oligodendroglial differentiation. Since few studies have detailed its genomic profile we performed an integrated genomic and transcriptomic analysis.
Design: Eight (7 primary, 1 secondary) GBM-Os previously characterized for *EGFR*, *PTEN*, *IDH1* and 1p and 19q status were selected. Formalin-fixed paraffin embedded tissue sections were macrodissected to maximize tumor percentage. All samples underwent SNP-CN analysis using Illumina CytoSNP arrays, targeted DNA sequencing using the Ion Torrent AmpliSeq Cancer Panel and a standard 48 mutation SNaPshot panel, as well as RNA-Seq using NuGen Ovation library prep and Illumina HiSeq2000 sequencing.
Results: SNP-CN array analysis identified chr 7 amplifications in all FISH-detected *EGFR* amplified cases in addition to a single case negative by FISH. Chr 10 and 9p loss occurred in 5/6 and 4/6 cases with *EGFR* amplification, respectively. 1p/19q codeletion was noted in 2/2 cases with the R132H *IDH1* mutation. Targeted sequencing of 16 genes mutated in GBMs identified 25 non-synonymous single nucleotide variations. The majority of GBM-Os exhibited mutations in *alpha thalassemia/mental retardation syndrome X-linked* (*ATRX*) (6/8). Other mutations of note occurred in *IDH1, PDGFRA*, *FUBP1, PIK3CA, MET, TP53, NOTCH1, EGFR*, and *ARID1A*. Unsupervised clustering of gene expression data demonstrated segregation of cases based on R132H *IDH1* mutation and *EGFR* amplification status, and the expression levels of several genes were uniquely associated with these groups. *EGFR* amplified tumors significantly overexpressed *AE binding protein 1* (*AEBP1*), a putative transcriptional repressor reportedly overexpressed in other GBMs. *IDH1* mutated cases significantly overexpressed the tyrosine kinase receptor *EPH receptor B1* (*EPHB1*), also consistent with previous reports.
Conclusions: This data indicates that combinations of SNP-CN arrays, targeted or modified exome DNA-Seq and RNA-Seq are informative tools in characterizing malignant brain tumors. Although morphologically distinct, this study demonstrates patterns of genetic alterations in GBM-O are similar to those in conventional GBM. As such, GBM-Os may be molecularly categorized based on amplifications of chr 7 and *IDH1* mutation status, which are significantly predictive of unique gene expression profiles.

1794 Expression of GATA3 in Brain Metastases of Breast Origin

N Hosseini, Z Ghorab, J Keith, E Slodkowska, F-I Lu, G Han, W Hanna, S Nofech-Mozes. Sunnybrook Health Sciences Centre, Toronto, ON, Canada.

Background: GATA3 expression has been associated with luminal type breast cancer and improved survival. Previous studies focused on the expression of GATA3 in primary breast carcinoma, but data on its expression in metastatic disease is limited. Brain metastases may be the presenting site in breast cancer or the only site of recurrence, particularly in triple negative disease. This study aimed to determine the proportion of metastatic breast carcinomas to the brain that express GATA3 and the association between GATA3 expression and the molecular subtypes in the setting of metastatic brain carcinoma of breast origin.
Design: All brain metastases resected in our institution between 1999- 2013 were identified from the Anatomic Pathology departmental database. Cases where breast origin was favored given the available immunohistochemical profile and considering the clinical setting were included in this study. Tissue microarray was constructed using 1 mm cores in triplicates and studied by immunohistochemistry for GATA3 (sc-268; Santa Cruz Biotech, Santa Cruz, CA), ER, PgR and HER2 (SP1, IE2, 4B5, respectively; Ventana Medical Systems, Tucson AZ, USA). HER2 gene amplification was determined by INFORM HER2 DNA and Chromosome 17 (both by Ventana Medical Systems, Tucson AZ, USA).
Results: Among 53 cases of metastatic breast cancer to the brain with available tissue blocks, GATA3 was expressed in 35 (66%) cases. The distribution among the different molecular subtypes is shown in Table 1.

Molecular subtypes:	Definition:	Number of cases:	GATA3 positive (%):
Luminal A-like	ER+/HER2-	14	9 (64)
Luminal B-like	ER+/HER2+	15	15 (100)
HER2-like	ER-/HER2+	15	10 (66)
TN-like	ER-/PR-/HER2-	9	1* (11)

*Weak, focal staining.
Conclusions: GATA3 is expressed in two thirds of brain metastases of breast origin and is strongly associated with luminal and HER2+ subtypes. In this setting, it can be used as an adjunct test supportive of breast origin. However; identifying the primary site in triple negative metastatic tumors continues to pose a challenge.

1795 Clinical and Biological Significance of the Intratumor Heterogeneity of PTEN Expression and Its Molecular Gene Alterations in Glioblastomas

MA Idoate, J Echeveste, R Diez-Valle, J Gallego, MD Lozano, JL Solorzano. University of Navarra, Pamplona, Navarra, Spain.

Background: Glioblastomas (GB) are characterized by a marked phenotypic and molecular heterogeneity. PTEN is a relevant multifactorial supressor gene that can be inactivated by deletion, mutation or promoter methylation. According to the immunostaining against PTEN, GB can be divided in homogeneous (diffusely positive) and heterogenous (positive and negative areas) tumors. The clinical and biological significance of this heterogeneity for PTEN expression and its molecular gene alterations has so far received little attention.
Design: A comparative study on paraffin and frozen samples from sixty consecutive GB was obtained. Clinical record was carried out in all cases. According to PTEN immunostaining paraffin-embedded GB were divided into homogeneous and heterogeneous tumors. DNA was extracted of microdissected samples from immunostained representative areas. Several relevant inactivation mechanisms of PTEN gene including LOH of 10q23 (PTEN region), hypermethylation status by PCR-MSP and mutation by direct sequencing, were studied and correlated with overall survival. Appropriate statistical tests were applied.
Results: PTEN protein expression was heterogeneous in 42 cases and homogeneous in 18. No correlation between PTEN expression and LOH of 10q23 status was observed in homogeneous GB. In the heterogeneous GB, LOH of 10q23 was found more frequently in the PTEN-positive areas (81%) than in the negative ones (35.7%, $p<0.001$). Only in two cases PTEN methylation was identified which corresponded to homogeneous GB. Mutation was only observed in 13 heterogeneous GB and did not correlate with immunostaining. In the Cox multivariate test, both heterogeneity and LOH 10q23 were not associated with age. For all cases, the overall survival for LOH of 10q23 status was significant (Log Rank, $p=0.005$). The median of overall survival was 421 days for homogeneous GB and 293 days for heterogeneous ones, being statistically significant (Log Rank, $p=0.014$). The tumors which showed both heterogeneity and LOH of 10q23 had a statistically significant worst prognosis with a median of overall survival of 237 days in respect to the homogeneous tumor without LOH (526 days; Log Rank, $p=0.003$).
Conclusions: The study of heterogeneity of PTEN expression and the LOH of 10q23 considered either isolated or combined have prognostic significance in GB. This heterogeneity of PTEN should be considered in the molecular studies of GB.

1796 Aberrant Alternative Splicing of DPF2 (BAF45D) in the Maintenance of an Undifferentiated Cellular State in Glioblastoma

MA Idoate, M Gonzalez-Huarriz, G Aldave, J Echeveste, S Tejada, F Pastor, A Rubio, A Aramburu, E Xipell, M Alonso. University of Navarra, Pamplona, Navarra, Spain; CEIT. University of Navarra, Pamplona, Navarra, Spain.

Background: Alternative splicing plays a key role in determining tissue-specific differentiation patterns. Interestingly, DPF-2 (BAF45d) is known as a tumor suppressor gene in the context of the SWI/SNF complex and plays a key role in the development of brain. Changes in splicing have been implicated in cancer. The objective of this study was to determine whether aberrant alternative splicing could play a role in the malignant phenotype of GB.

Design: We identify DPF-2 as differentially splices in three paired normal/GB patients samples and a commercial normal brain RNA using splicing arrays (HJAY J array, Affimetrix). After, we validated our results with conventional PCR and qRT-PCR in 20 GB surgically resected by 5-ala fluorescence, 10 low grade astrocytomas, and 5 normal brain controls. The fluorescent was used to take biopsies from the tumor center (red areas), and from adjacent periphery (blue areas). We performed loss and gain of function studies using MTT assays, cell cycle analyses (viability and proliferation) and immunofluorescence-qRT-PCR (differentiation) in established gliomas cell lines (U87 MG and NSC11) and in early postnatal murine neural precursors.

Results: We found that DPF-2 presented a differential alternative splicing in GB when compared with periphery, normal brain tissue or low grade samples. The differential alternative splicing in the periphery was similar to the normal brain tissue and low-grade astrocytomas and different to the center samples in all cases. We validated this results with a published exon array study (6 normal brain samples and 26 GB). In addition, established gliomas cell lines presented the tumor spliced isoform. The inhibition of the tumoral DPF-2 isoform resulted in a significative reduction in proliferation and in morphology changes towards a more differentiated phenotype in GB cell lines. Interestingly, DPF2 tumoral isoform was the predominant transcript in early postnatal murine neural precursors and its expression disappeared as these cells were instructed towards neurons.

Conclusions: Our results suggest that the alternative splicing of DPF-2 in GB could participate in the maintenance of an undifferentiated cellular state. In addition, our data suggest that alternative splicing is a mechanism that could be central to GB development.

1797 CHARGE Syndrome: Neuropathological Update

G Juric-Sekhar, JR Siebert, RF Hevner. University of Washington, Seattle, WA; Seattle Children's Hospital, University of Washington, Seattle, WA.

Background: CHARGE syndrome is a rare, usually autosomal dominant condition characterized by 3C triad (Coloboma-Choanal atresia-abnormal semicircular Canals), arhinecephaly, rhombencephalic dysfunction, retardation of growth and/or development, and dysmorphic features. A causative gene called *CHD7*, which is involved in controlling the expression of many other genes, has been identified and accounts for at least 2/3 of cases. 55-85% of patients with CHARGE syndrome have CNS abnormalities including holoprosencephaly, dysgenesis of the frontal lobes, agenesis of the septum pelucidum, nodular heterotopias, lissencephaly, vermian hypoplasia or stenosis of Sylvius aquedact. However, the spectrum of gross and microscopic abnormalities has remained incompletely defined in CHARGE syndrome.

Design: This study reports a series of postmortem neuropathological examination of three patients with CHARGE syndrome including detailed findings, and one with known mutations in the *CHD7* gene.

Results: The most common findings included hypoplastic olfactory bulbs (2/3) and arhinencephaly (1/3), microcephaly with hypoplastic frontal lobes with no gyral abnormalities, and cerebellar heterotopia. Other features included hypoplastic optic nerves, early depletion of external granular layer, and heterotopic granular layer in dorsolateral pontine surface. The cranial nerve VII and VIII were histologically examined in one patient, and no histological abnormalities were observed. The spinal cord appeared unremarkable.

Conclusions: This study indicates that CNS abnormalities in CHARGE syndrome are heterogeneous and appear to involve multiple developmental mechanisms including patterning, proliferation, and cell migration. These abnormalities provide clues to the underlying molecular and developmental mechanisms causing the brain malformations seen in CHARGE syndrome.

1798 Translational Impact of Glioblastoma Cancer Stem-Like Cells

LM Larocca, L Ricci Vitiani, QG D'Alessandris, T Cenci, M Martini, R De Maria, R Pallini. Università Cattolica del Sacro Cuore, Rome, Italy; Istituto Superiore di Sanità, Rome, Italy; Istituto Nazinale Tumori Regina Elena, Rome, Italy.

Background: Cancer stem-like cells (CSC) are thought to represent the population of tumorigenic cells responsible for tumor initiation, development, and recurrence. We conducted a prospective study to explore the prognostic potential of CSC analysis in glioblastoma (GBM) patients.

Design: We investigated the relationship between the in vitro growth potential of CSCs and outcome in 139 consecutive GBM patients treated with complete or partial tumor resection followed by radiotherapy combined with temozolomide (TMZ) treatment. We also evaluated the molecular profile of the parent tumor along with in vitro growth features of CSCs in order to establish any translational impact of CSCs cultures.

Results: Out of 139 GBM tumor samples, 40 of them (28.8%) generated cell cultures that grew as free-floating spheres in serum-free medium and showed all the biological landmarks of CSCs. In vitro generation of CSCs negatively correlated with overall survival of patients (P = 0.0033, log rank test). A poor overall was observed among patients whose tumors generated CSCs and showed unmethylated MGMT promoter (P = 0.0176). Tumors generating CSCs and expression EGFRvIII trended towards worse outcomes (P = 0.0783). Taking into account clinical variables, including age, KPS, tumor location, surgery type, pathological and molecular features, including Ki67, MGMT promoter methylation, expression of EGFRvIII, PTEN, and VEGF, and generation of CSCs, KPS<70 and CSCs generation emerged as significant independent prognostic factors (P = 0.0111 and 0.0160, respectively). Analyses of clonogenicity, VEGF isoforms, and resistance to radiation and TMZ, suggest that CSCs may play multiple roles in GBM biology.

Conclusions: The generation of CSCs identifies a subgroup of GBM tumors with worse prognosis. In vitro analysis of CSCs represent a powerful tool to tailor targeted therapies to treat GBM patients.

1799 WHO Criteria Act Synergistically to Influence Clinical Outcome in Grade II Meningiomas

SE Martin, SA Wagner, EM Hattab. Indiana University School of Medicine, Indianapolis, IN.

Background: WHO grade II designation of meningiomas may be achieved using any of the five currently defined criteria:≥4 mitoses/10 HPFs, brain invasion, clear cell morphology, chordoid morphology, or≥3 "soft" criteria (necrosis, hypercellularity, small cell change, prominent nucleoli, sheeting architecture). Under the present guidelines, whether a meningioma shows one or more of these criteria has no bearing on the final grade of the tumor or the implied prognosis. We hypothesize that meningiomas with two or more grade II qualifying criteria may behave worse than those with only one.

Design: Our pathology archives were searched for grade II meningiomas from 1986 to 2008. One hundred twenty-five cases that qualify as grade II by 2007 WHO grading criteria were obtained. Cases were evaluated for various clinical and pathologic parameters, and depending on the number of grade II-qualifying criteria present, cases were placed into one of three groups: 1 for those with 1 criterion (n=58), 2 for those with 2 (n=45), and 3 for those with 3 or more (n=22).

Results: Kaplan Meier analysis demonstrated statistically significant differences in recurrence-free survival (RFS) and overall survival (OS) between the groups (log rank overall comparisons: RFS P=.028; OS P=.04). Pairwise comparisons using the Mantel-Cox log rank test showed statistically significant differences in recurrence free survival and overall survival between groups 1 and 3 (RFS P=.015; OS P=.028) and between groups 2 and 3 (RFS P=.022; OS P=.026). 14%, 11%, and 46% of patients in groups 1, 2, and 3 respectively died of their disease (P=.014).

Conclusions: Our study shows that meningiomas having only one or two grade II criteria behave significantly better than those with three or more, suggesting that not all grade II meningiomas are created equal. While patients with WHO grade III meningiomas almost universally receive adjuvant radiation therapy, whether or not a patient with grade II meningioma receives adjuvant radiation therapy is often institution dependent, reflecting the lack of consensus on how to manage these patients. While additional studies are required, our results do suggest that there is an added benefit to further stratifying grade II meningioma patients in a way that may directly impact their treatment decisions.

1800 "Neural" Morphology and Merlin and Neurofibromin Immunoreactivity Distinguish NF2-Associated Meningiomas from Sporadic Ones

SE Martin, AL Wiens, EM Hattab. Indiana University School of Medicine, Indianapolis, IN.

Background: Neurofibromatosis II (NF2) is an inherited tumor syndrome that predisposes patients to schwannomas, ependymal tumors, and meningiomas. Schwannomas and meningiomas tend to be multiple in patients with NF2, while sporadic tumors tend to be solitary. Prior studies have suggested that, compared to sporadic tumors, NF2-associated meningiomas may have a higher frequency of atypical morphologic features, including higher proliferative activity and prominent nuclear atypia.

Design: We examined 16 meningiomas from 9 NF2 patients and compared them with 18 sporadic meningiomas from 18 age-matched patients. Tumors were categorized according to established 2007 WHO criteria for classification of brain tumors and were examined for various histologic parameters including atypical features, "neural" appearance, and intratumoral inflammatory infiltrates. Tissue microarrays were constructed, and immunohistochemical stains for neurofibromin, merlin, IMP3, progesterone receptor (PR), S100 protein, and Ki67 were performed. A standard t test was used to analyze continuous data. Chi-square tests were utilized to compare categorical morphologic and immunohistochemical parameters. Each stain was scored for extent of immunohistochemical expression (percentage of cells staining) and staining intensity, except for Ki67, which was reported in percentages only.

Results: There were no statistically significant differences in age or gender, indicating appropriate matching of NF2 and sporadic meningiomas. Meningiomas from NF2 patients were more likely to have a "neural" or "onion-bulbing" appearance (P<0.01), had significantly greater merlin expression (P=0.04), and showed significantly higher neurofibromin staining intensity (P<0.01). There were no significant differences between NF2 and sporadic meningiomas with regard to histologic grade (11 were WHO grade I and 5 were grade II) or other morphologic parameters, expression pattern for PR and IMP3, or Ki67 proliferative index.

Conclusions: Parameters that may aid in distinguishing NF2-associated meningiomas from sporadic ones include immunohistochemical staining for merlin and neurofibromin as well as "onion-bulbing" morphology.

1801 Reliability of Somatostatin Receptor 2a as a Marker of Meningioma: An Immunohistochemical Study

JR Menke, AM Gown, S Thomas, A Perry, T Tihan. UCSF, San Francisco, CA; PhenoPath, Seattle, WA.

Background: Meningioma is the most common extraaxial primary CNS tumor. While most meningiomas are easily diagnosed on routine stains, immunohistochemistry may become necessary for diagnosis in some tumors. However, a robust immunohistochemical marker has been elusive. Currently the most reliable meningioma markers are epithelial membrane antigen (EMA) and progesterone receptor (PR). Recent studies suggest somatostatin receptor 2a (SSTR2a) may also be a good meningioma marker.

Design: We identified cases of meningioma with an unequivocal diagnosis and WHO grade at our institution between 2002 and 2012. Small biopsy material and decalcified or frozen tissues were excluded. Slides were reviewed for diagnosis and selection of the appropriate block for microarray generation. Two 2 mm cores were taken from each block to generate microarrays along with control tissue from normal meninges, normal brain, lung adenocarcinoma and placenta. Immunohistochemical stains for SSTR2a, EMA and PR were performed following optimization of pretreatment and primary antibody dilutions. Each tissue core was assigned a score (0 to 3+) indicating signal intensity. The Mann Whitney Wilcoxon test was used determine whether each marker showed significantly different score distributions between normal meninges and meningiomas.

Results: 176 cases were included in the study. SSTR2a was positive in all 176 cases, EMA was positive in 168 cases and PR was positive in 171 cases. The differences in staining among normal meninges, meningioma and lung adenocarcinoma were analyzed. SSRT2a was most striking in its ability to stain positively for meningiomas as opposed to controls ($p < 6.3$ e-7), followed by EMA ($p < 4.8$ e-6) and PR ($p < 0.01$). The interquartile ranges of different factors' scores (Figure 1) showed that SSTR2a is the most reliable marker for meningiomas and that normal meninges were essentially negative for this marker.

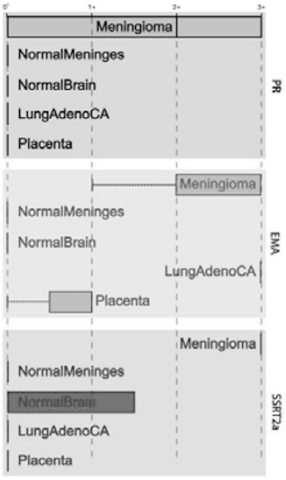

SSTR2a was positive in 5 cases, in which both EMA and PR failed to stain tumor.

Conclusions: SSTR2a appeared to be a robust marker for meningiomas and even stained some meningiomas that classical markers did not. Studies are underway to determine SSTR2a staining in schwannomas, solitary fibrous tumors and other mesenchymal neoplasms to further characterize the specificity of this marker.

1802 Clinical and Molecular Analysis of Glioblastoma with Oligodendroglial Component

JK Myung, HJ Cho, HN Kim, S-H Park. Seoul National University Hospital, College of Medicine, Seoul, Republic of Korea.

Background: Glioblastoma (GBM) is the most common primary brain tumor in adults. GBM has several histological variants; however, the biological and genetic characteristics of each variant are largely unknown. Among them, GBM with oligodendroglioma component (GBMO) is a newly adopted variant of GBM in the updated 2007 World Health Organization (WHO) classification of tumors of the central nervous system (CNS).

Design: We investigated a series of 35 patients. And we evaluated the amplification of the *EGFR* gene, homozygous deletion of 9p21.3, allelic loss of 1p19q, the *BRAF* mutation, and *MGMT* promoter methylation according to *IDH1*[mutation status (mutant vs. wild type).

Results: The mean age of the mutant *IDH1* group was significantly younger than the wild-type *IDH1* group (43.9 years [range, 19–62 years] vs. 59.4 years [range, 31–77], $p < 0.05$). The frequencies of the *EGFR* gene abnormality and 9p21 homozygous deletion were significantly higher in the wild-type *IDH1* group than in the mutant *IDH1* group. On the contrary, the incidence of *MGMT* promoter methylation was significantly higher in the mutant *IDH1* group than in the wild-type *IDH1* group ($p < 0.05$). The 1p19q co-deletion was rare in both groups. Most patients in the wild-type *IDH1* group (19/20) had primary GBMO; however, 64.3% (9/14) of patients in the mutant *IDH1* group had secondary GBMO. Kaplan-Meier survival analysis revealed that the cumulative survival rate of GBMO at our institute was worse than that of WHO grade II and III astrocytic and oligodendroglial tumors at our institute, but was similar to that of conventional GBM. Interestingly, there was no survival difference between primary and secondary GBMO or between mutant *IDH1* and wild-type *IDH1* GBMO.

Conclusions: In our study, as we expected, there were primary and secondary GBMOs. Primary GBMO occurred in patients of older age than secondary GBMO, which had a high frequency of *EGFR* amplification and 9p21.3 homozygous deletion and a simultaneously low frequency of *IDH1* mutation and *MGMT* promoter methylation. Secondary GBMO occurred in patients of younger age than did primary GBMO, which showed a low frequency of *EGFR* amplification and 9p21.3 homozygous deletion and a high frequency of the *IDH1* mutation and MGMT promoter methylation. In terms of survival, the cumulative survival rate of GBMO was similar to that of conventional GBMO but much worse than that of grade II and III astrocytic and oligodendroglial tumors.

1803 Clinicopathological Features of Brain Metastases from Ovarian Carcinoma: A Case Series and Diagnostic Approach

H Nafisi, M Cesari, J Karamchandani, J Keith. Department of Anatomic Pathology, Sunnybrook Health Sciences Centre, University of Toronto, Toronto, Canada; Department of Pathobiology and Laboratory Medicine, St. Michael's Hospital, University of Toronto, Toronto, Canada.

Background: While brain metastasis remains a rare manifestation of ovarian epithelial carcinomas, there has been an increasing number of reported cases in recent years.

Design: We present clinicopathological characteristics of 12 consecutive cases of brain metastases from ovarian epithelial carcinoma diagnosed at two academic institutions.

Results: The mean age at diagnosis of ovarian carcinoma and their subsequent brain metastases were 54.7 and 58.3 years, respectively. The case series included 7 patients with high-grade serous carcinoma, 2 with clear cell carcinoma and a single case each of carcinosarcoma, mucinous and high-grade adenocarcinoma. The majority of patients were advanced stage at initial diagnosis. Neuroimaging features showed half of the patients to have multiple brain metastases, most were ring enhancing, and the most common sites were frontal lobe followed by cerebellum.

Conclusions: We present a case series of brain metastases from ovarian epithelial carcinomas. As neuropathologists may have little experience in dealing with these neoplasms, we describe the pathological features of the most common ovarian epithelial carcinomas metastasizing to the brain and provide recommendations to neuropathologists to aid in their recognition and proper classification.

1804 SOX10 Is Superior to S100 in the Diagnosis of Meningioma

J Ng, A Celebre, D Munoz, JL Keith, J Karamchandani. McMaster University, Hamilton, ON, Canada; University of Toronto, Toronto, ON, Canada.

Background: Meningiomas and schwannomas are primary tumors of the central nervous system that can show overlapping morphology - a similarity most conspicuous in the fibrous variant of meningioma(f_meningioma), which typically shows poor 'whorl' formation. S100 is the most commonly employed immunohistochemical(IHC) stain used to evaluate neural crest differentiation, potentially leading to misclassification as up to 70% of f_meningioma can express S100. We aimed to determine if Sox10 would prove a more specific alternative to S100 in such cases.

Design: We compared the mRNA expression of S100B and SOX10 using the NCBI GSE16581 meningioma dataset. With IHC we evaluated 19 cases of f_meningioma using full cross-sections(FCS), and 147 cases of WHO grade I meningiomas (all subtypes) using tissue microarrays (TMA)-2 cores from each tumor. 2 comercially available Sox10 antibodies from Cell Marque(CM) and Santa Cruz(SC) were tested.

Results: Unlike in tumors of neural crest origin, in meningeal tumors SOX10 and S100B showed no correlation in expression($r=-0.002$, $p=0.989$).

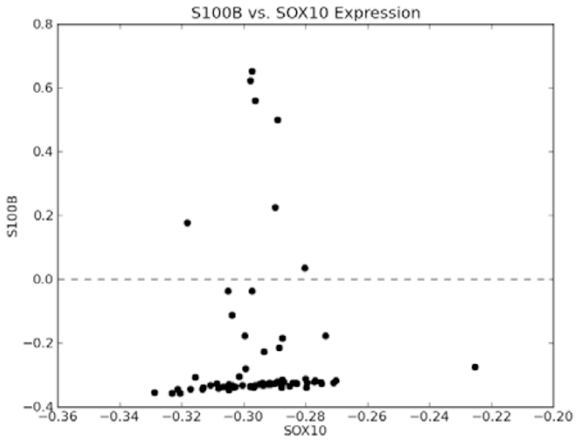

By IHC Sox10 was concordant between the 2 TMA spots in 99% of cases. S100 was concordant in 93% of cases. S100 was positive in 14/19(73.7%) of f_meningioma FCSs and 71/147(48.3%) of TMA tumors, while Sox10 was positive in only 1/19(5.3%) of FCSs and 3/147(2.0%) of TMA tumors.

Table 1: Summary of IHC staining

		# Positive					
		S100		Sox10			
		Focal	Diffuse	Focal		Diffuse	
	N			CM	SC	CM	SC
TMA	147	53/147(36%)	18/147 (12%)	0	0	3/147(2%)	0
FCS	19	7/19(38)%	7/19 (38%)	NA	1/19(5%)	NA	0

The majority of S100 positive tumorswere Sox10 negative (Figure 2).

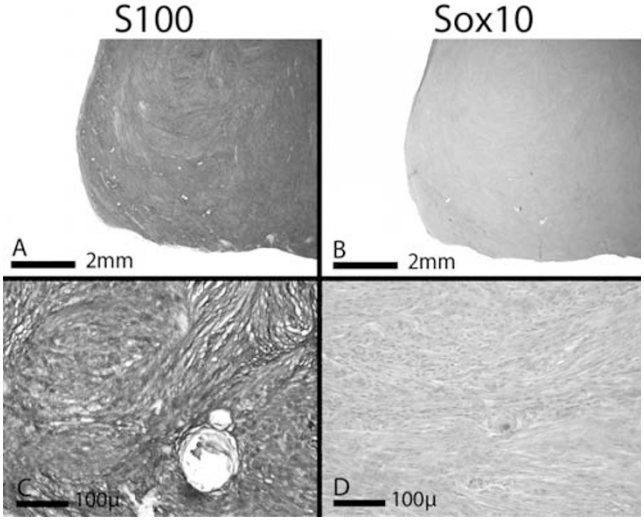

The CM antibody stained 3 TMA cases diffusely (all were negative with the SC antibody). The antibody from SC stained 1 case of f_meningioma focally. It is unlikely these results are a consequence of random sampling (binomial proportions p-value<2.2e-16).

Conclusions: Sox10 is superior to S100 in the differential diagnosis of schwannoma and meningioma.

1805 Pituitary Adenoma-Neuronal Choristoma: A Spectrum of Neuronal Differentiation of an Adenoma

MT Nguyen, E Lavi. New York Presbyterian, Weill Cornell Medical College, New York, NY.

Background: The presence of neuronal elements within a pituitary adenoma, although rare, had been recognized as early as 1926 and has been named hamartoma, choristoma, gangliocytoma, or most recently pituitary adenoma-neuronal choristoma (PANCH). Signs of neuronal differentiation of typical pituitary adenomas had been previously suggested. However, the origin, the extent of its presence, and the relationship of these neuronal elements to the pituitary adenoma remain uncertain. We proposed that the presence of neuronal elements in PANCH is not the result of two pathobiological processes but rather a spectrum of neuronal differentiation of an endocrine neoplasm that consists of both neuronal and endocrine properties.

Design: A prospective study was performed on 33 consecutive cases of pituitary neoplasms (adenomas, invasive adenomas, and carcinoma) at our institution from 10/2011-5/2012. Two cases of PANCH were included as controls. Examination of the H&E and immunohistochemical stains including synaptophysin (SYN), pituitary hormones, Ki-67, hexaribonucleotide binding protein-3 or neuronal nuclei antigen (NeuN), and neurofilament (NF) were performed on all cases.

Results: All 33 cases of pituitary neoplasm demonstrated diffuse positivity for SYN and variable staining of hormone markers, consistent with the diagnosis of pituitary adenoma. Nine of 33 (27.3%) cases showed variable nuclear staining for NeuN ranging from 5% of the adenoma cells in one case and up to 90% in another. Light microscopy of the H&E revealed no distinctive histologic features between the adenoma cells that were immunoreactive for NeuN and those that were not immunoreactive. The two cases of PANCH consisted of two distinct mixed populations of cells. The cells corresponding to ganglions histologically were strongly positive for NF and NeuN. A small population of the adenomatous cells (~30%) were also positive for NeuN and few (<20%) were positive for NF.

Conclusions: The presence of ganglion cells in pituitary adenoma, sometime referred to as PANCH, is the result of neuronal differentiation of adenomatous cells that consist of both endocrine and neuronal properties. The results of this study demonstrate that adenomatous cells of pituitary adenoma clearly contain an innate neuronal epitope as highlighted by NeuN stain, which is a highly specific marker of differentiated neuronal cells. This further supports our theory that a PANCH is a continuum of a pituitary adenoma rather than a distinct tumor and should be labeled as pituitary adenoma with ganglionic differentiation.

1806 Mitotic Index Using Phosphohistone H3 (pHH3) Is Predictive of Recurrence-Free Survival in Meningiomas

A Olar, KM Wani, EP Sulman, A Mansouri, G Zadeh, CD Wilson, KD Aldape. University of Texas MD Anderson Cancer Center, Houston, TX; University of Toronto, Toronto, ON, Canada.

Background: Meningiomas are the most common primary CNS tumors and are graded into three subgroups predictive of recurrence. The WHO grading criteria are in large part based on mitotic counts per 10 high power fields but there is great within-grade variation of recurrence risk. Histone H3 phosphorylated at serine 10 (pHH3) is a sensitive marker for mitotic figure detection and allows the determination of a mitotic index (number of mitoses per 1000 tumor cells) which could add prognostic information to predict recurrence-free survival (RFS).

Design: A set of 319 meningiomas were stained with pHH3 (S10) (anti-rabbit, Cell Signaling Technology, Inc.). The highest mitotically-active area was identified and the pHH3 score calculated as number of mitotic figures per 1000 tumor cells. Univariate and multivariate survival analyses were performed with variables that included RFS, WHO and Simpson grades.

Results: The median RFS among WHO grade I (n=227), II (n=82), and III (n=10) cases were 675, 375, 106 weeks ($p< 0.01$) and the median pHH3 indices were 1, 3, and 14.5, respectively. As a categorical variable, distinct risk groups were identified using 0-2, 3-7, and greater than 7 mitotic figures, respectively, with median RFS in these 3 groups of 683, 430, and 130 weeks respectively ($p<0.01$). On univariate analyses, WHO grade, and Simpson grade were also predictive of RFS ($p<0.01$). On multivariate analysis mitotic index ($p<0.01$) was significantly associated with RFS after adjustment for Simpson grade and WHO grade. Interestingly, among the 82 grade II meningiomas, mitotic index segregated RFS risk groups ($p<0.01$, see Figure), suggesting that pHH3 determination may add information to WHO grade in prediction of recurrence.

Conclusions: Mitotic index, as defined by pHH3-positive mitoses per 1000 tumor cells, was highly predictive of recurrence in meningioma. Its role in clinical practice should be considered, especially in WHO grade II tumors to stratify recurrence risk and potentially to guide adjuvant therapy.

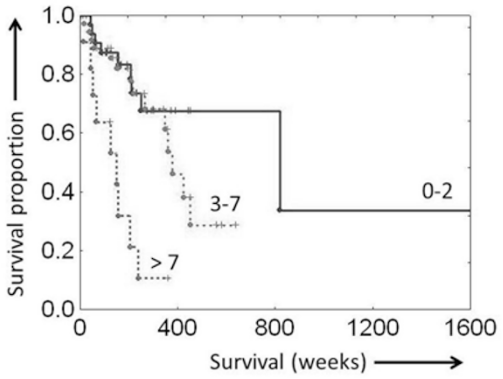

1807 Is Neurodegeneration a Consequence of Temporal Differences in the Induction of Protective Markers GDNF and NO? A Cell Culture and Organ Failure Animal Study

A Padilla, M-F Doursout, BJ Poindexter, DLM Hickson-Bick, RJ Bick. University of Texas Medical School, UT Health, Houston, TX.

Background: Neurodegenerative diseases have a devastating toll on aging populations in the US and throughout the world. There are numerous reports that neurodegenerative diseases are caused by inflammation. A Bacterial endotoxin (LPS) treated rat model that was previously published mimics many of the neuro-pathological changes associated with neurodegenerative diseases. In this model, we found increased concentrations of circulating cytokines, circulating nitric oxide (40 fold; NO), and tissue glial cell-derived neurotrophic factor (GDNF). We thus hypothesized, that the protective factors GDNF and NO might avert neurodegeneration due to inflammation in susceptible areas, such as in the olfactory bulb (OB).

Design: In our studies we used both cell cultures and animal models, with cells and tissues being probed for GDNF content and inducible (iNOS), endothelial (eNOS) and neuronal (nNOS) nitric oxide synthase using fluorescence deconvolution microscopy. Images were acquired, sections were stacked for the generation of full thickness models and quantifications of targeted markers were made.

Results: Both a microglial cell line and an astrocyte cell line synthesized GDNF and nitric oxide synthase and these products appeared in a time dependent manner and in specific areas of brains from LPS treated rats. In the cortex, eNOS content does not increase following treatment but is increased 8-fold in the OB (10268±4365 v 84598±11049 pixel density). The combined results suggest that neurodegeneration is initiated by inflammation prior to 'protective' mechanisms being available, and also at times when protective mechanisms are overwhelmed. This might result in a delay in cell loss, but does not avert subsequent catastrophic cell death and accompanying cell signaling disruptions.

Conclusions: Our findings suggest that protective syntheses of GDNF and NO might not coincide with the detrimental, degenerative episodes, and thus being only partially effective in protection and halting cell death. Our results suggest that cell death; in particular neurodegeneration is initiated by inflammation prior to the release of GDNF and NO. Although not all causative factors that contribute to these inflammation based diseases are known, studies like this can provide insight into their pathogenesis for the development of adequate therapy.

1808 Combinational Therapy of ABT-263 and GDC-0941 Exerts Synergistic Activity in Glioblastoma

F Pareja, L Greene, M Siegelin. New York Presbyterian Hospital, Columbia University, New York, NY.

Background: Glioblastoma multiforme (GBM) is the most common human brain neoplasm, has a devastating course and limited therapeutic options. One of the mechanisms why GBMs are not susceptible to current treatments is their intrinsic resistance to apoptotic cell death. GBMs display a deregulated apoptotic pathway with high levels of the anti-apoptotic Bcl-2 family of proteins and overt activity of the PI3K signaling pathway. Therefore, combined interference of the PI3K pathway and the Bcl-2 family of proteins might be a reasonable therapeutic strategy.

Design: ABT-263, an orally available Bcl-2 small molecule inhibitor, and GDC-0941, a phosphatidylinositol 3-kinase (PI3K) inhibitor, were used to treat LN229 (TP53 mutated, PTEN wild-type) and U373 (TP53 mutated, PTEN mutated) glioblastoma cells, alone or in combination. The 3-(4,5-dimethylthiazol-2-yl)-2,5-diphenyltetrazolium bromide (MTT) assay was performed to determine cellular viability after treatment. Annexin V/propidium iodide staining followed by flow-cytometry analysis was employed to examine apoptotic cell death. Expression of downstream proteins was determined by Western-Blotting.

Results: While GDC-0941 single treatment had a modest effect on cell viability, therapy with ABT-263, in the range of 1 to 8 μM, displayed a marked inhibition of cell viability and induction of apoptotic cell death. Moreover, combination treatment using ABT-263 and GDC-0941 showed a synergistic effect, with a further decrease in cellular viability as assessed by MTT assay. Consistently, combination treatment of ABT-263 and GDC-0941 resulted in a significant increase of Annexin V positive cells compared to single treatments. Therapy with GDC-0941 depleted ph-AKT (ser473) levels, lowering the threshold for the cytotoxic actions of ABT-263. Furthermore, the combination treatment led to enhanced cleavage of caspases.

Conclusions: The combination therapy of ABT-263 and GDC-0941 might be a novel therapeutic regimen that specifically targets aberrantly active, deregulated pathways in GBM, overcoming endogenous resistance to apoptosis.

1809 Differential Immunohistochemical Profiles of Malignant Peripheral Nerve Sheath Tumors and Cellular Schwannomas

M Pekmezci, A Horvai, A Perry. University of California San Francisco, San Francisco, CA.

Background: Cellular schwannoma (CS) is an uncommon but well-recognized benign nerve sheath tumor, frequently misdiagnosed as malignant peripheral nerve sheath tumor (MPNST). In this study, we explore potential diagnostic roles of SOX10, SOX2, p75NTR, p16, p53 and EGFR expression in this differential.

Design: We have reviewed all MPNST and CS cases diagnosed between 1990 and 2012 and reached to a consensus diagnosis. Outside consultation cases, neoplasms for which melanoma or other sarcoma diagnoses were not entirely ruled out, and nerve sheath tumors with equivocal features of malignancy were excluded. Clinical data were retrieved from electronic medical records. Continuous variables were compared with Mann-Whitney U, and categorical variables were compared with Fisher's Exact tests. After Bonferroni correction, variables with p-values <0.0083 were considered as potentially useful.

Results: Forty MPNST and 12 CS cases were included in the study. There was no recurrence, no metastasis and no disease-specific deaths among CSs. Five-year progression-free survival rates were 100% and 33.2%, and five-year disease-specific survival rates were 100% and 34.6% for CS and MPNST, respectively (p=0.005 and p=0.0013, respectively). Morphological and immunohistochemical findings are summarized in table 1.

Clinical, Morphologic and Immunohistochemical Findings

	MPNST (n=40)	CS (n=12)	p
Male	17	6	0.75
Age, median (range)	37.5 (11.2-71.8)	44.7 913.8-70.3)	0.14
Neurofibromatosis 1	25	0	<0.0001
Size, cm, median (range)	8.8 (0.5-26)	4.8 (1-9.8)	0.005
Fascicles	39	6	0.001
Whorls	2	7	0.0002
Intravascular bulging	20	2	0.04
Angiocentricity	19	1	0.014
Capsule	3	5	0.011
Macrophages	0	4	0.002
Necrosis	31	2	0.0003
Maximal mitotic index, per 10 HPF, median (range)	25 (1-90)	5.5 (1-10)	<0.0001
S100	21	12	0.002
Diffuse S100	4	11	<0.0001
SOX10	10	12	<0.0001
Diffuse SOX10	0	7	<0.0001
p16	17	12	<0.0001
EGFR	29	0	<0.0001
p75NTR	32	7	0.13
SOX2	31	11	0.26
p53	30	10	0.43
Ki67, % median (range)	60 (2-90)	20 (3-50)	<0.0001

MPNST: Malignant peripheral nerve sheath tumor; CS: cellular schwannoma, HPF: High-power field

Conclusions: In our study, a well-defined capsule, macrophage-rich areas, and cellular whorls favored CS, while intersecting fascicles, intravascular protrusions, perivascular hypercellularity, necrosis, and mitotic index >10/10 high-power field favored MPNST. EGFR immunoreactivity and losses of S100, SOX10 and p16 expression were nearly exclusively seen in MPNST; as such, these potentially useful diagnostic markers should be further validated in larger series and applied to problematic tumors where the distinction between CS and MPNST is less clear.

1810 Patterns of INI1 Expression in Malignant Peripheral Nerve Sheath Tumor, Cellular Schwannoma and Synovial Sarcoma

M Pekmezci, AE Horvai, A Perry. University of California San Francisco, San Francisco, CA.

Background: Loss of INI1 protein expression has been reported in multiple neoplasms with a continuously growing list. A unique pattern of decreased expression was reported as a specific and relatively sensitive marker in synovial sarcoma (SS) as compared to its histologic mimics including malignant peripheral nerve sheath tumor (MPNST). Another unique pattern of INI1 expression was mosaic staining, which was previously reported in syndrome-associated schwannomas. In this study we investigated the INI1 expression patterns of SS, MPNST and cellular schwannomas (CS) because distinguishing among these three neoplasms often presents a diagnostic challenge.

Design: Pathology archives were searched for SS, MPNST and CS cases, and clinical data was retrieved from electronic medical records. Fifty-five SS with genetic confirmation, and 49 peripheral nerve sheath tumors (37 MPNST and 12 CS), all lacking *SS18* gene arrangement were included in the study. We evaluated the intensity and distribution of INI1 expression by immunohistochemistry on tissue microarrays.

Results: Among SS, 14 (25.5%) had diffuse strong INI1 expression, 2 (3.6%) were mosaic, 29 (52.7%) showed diffuse weak INI1 expression, and 3 (5.5%) had complete loss of INI1 expression. The remaining 7 biphasic SS showed variable patterns in spindled and epithelioid regions. One featured complete loss in the spindled cells and diffuse strong expression in epithelioid cells. Five had complete loss in spindled cells, with reduced expression in epithelioid foci, and one case retained diffuse strong expression in the spindle cell component but reduced expression in epithelioid cells. In contrast, neither reduced nor complete loss of expression was seen in nerve sheath tumors. Four CS (33.3%) and 10 MPNST (27%) showed mosaic staining. We observed no correlation between INI1 expression and neurofibromatosis 1 status among MPNST cases.

Conclusions: Whereas reduced INI1 expression was specific for SS, mosaic expression was observed in MPNST and SS. Thus mosaic expression should not be used for diagnostic distinction between SS and MPNST. Our data suggest that INI1 expression should be interpreted cautiously when approaching the differential diagnosis of SS, MPNST and CS.

1811 Lanthionine Ketimine-Ethyl Ester Increases the Haploinsufficient Tumor Suppressor Beclin-1, to Slow Glioma Growth

J Purdy, A Hristov, K Venkova, R Towner, K D'Rummo, S Lowenstein, M Rohs, K Hensley. University of Toledo Health Science Center, Toledo, OH; Oklahoma Medical Research Foundation, Oklahoma City, OK.

Background: Beclin-1 (BECN1) is a haploinsufficient tumor suppressor that is commonly deleted in glioma. Beclin-1 is a prognostic factor in human gliomas, with low protein expression correlated to shorter lifespan and higher tumor grade. Beclin-1 may regulate tumorigenesis through its action as a master autophagy control protein. Our laboratory has recently discovered a brain amino acid metabolite called lanthionine ketimine (LK) with potent effects on neural and glial biology. A cell- and brain-penetrating lanthionine ketimine ester derivative (LKE) was found to increase autophagy markers in human SHSY5Y neuroblastoma cells and human A172 glioblastoma cells. Therefore studies were undertaken to determine whether LKE could affect beclin-1 in cell culture and in vivo; and whether the compound could slow glioma proliferation in vitro or in vivo.

Design: Cell culture studies: (A) Cultured SHSY5Y and A172 cells were treated with LKE over a broad dose range and for various times in order to assay effects on autophagy markers including LC3, p62/SQSTM1, and beclin-1. (B) In cell proliferation studies, A172 cells were cultured with LKE then challenged with the chemotherapeutic temozolomide and allowed to proliferate in the presence or absense of LKE. Proliferation was monitored by regular assay of cell number using a tetrazolium reduction assay. In vivo studies: (A) Sprague-Dawley rats were cortically implanted with 100,000 C6 glioma cells and tumor volumes measured at 21d post-implantation by magnetic resonance imaging (MRI). Animals received LKE either in the diet or by intraperitoneal daily injections. Control animals received vehicle only. (B) In related studies mice were administered a dietary LKE formulation chronically and beclin-1 assessed in cortical tissue.

Results: In cell culture experiments LKE increased beclin-1 protein, but not message, by 2-3 fold in SHSY5Y and A172 cells. The effect was dose and time dependent. LKE slowed A172 cell proliferation after temozolomide challenge. In vivo, LKE increased brain beclin-1 by up to 2-fold and significantly reduced C6 glioma volume in the implantation model.

Conclusions: Derivatives of the brain metabolite lanthionine ketimine promote autophagy, partly through a mechanism of increasing beclin-1, and slow glioma growth. These studies raise new questions about the natural biology of brain lanthionines and the potential of their derivatives as experimental therapeutics to slow brain tumor growth.

1812 Astrocyte Elevated Gene-1 (AEG-1) Copy Number Alterations and Protein Expression in Clinical Progression of Human Gliomas

HT Richard, JF Harrison, C Fuller. Virginia Commonwealth University, Richmond, VA.

Background: Gliomas are the most common primary brain tumor in all age groups. Despite advances in the elucidation of the molecular mechanisms of gliomagenesis and targeted therapies, treatment options are limited and morbidity remains high. Astrocyte elevated gene-1(AEG1), a potential therapeutic target, has been reported to be overexpressed in numerous tumor types including malignant gliomas. A recent study reported >90% gliomas had high expression of AEG1; however, the etiology of

this finding has not been fully elucidated. This study aims to determine the incidence of AEG1 copy alterations and protein expression in gliomas, with additional correlations sought regarding pathologic parameters and survival.
Design: Clinical and histologic data of 50 gliomas were reviewed and tissue microarrays(1mm cores) generated using an automated system(Beecher ATA-27). A rabbit polyclonal antibody to LYRIC(AEG1) was used for immunohistochemistry(Abcam, Ma USA); cases with moderate to intense cytoplasmic and/or nuclear staining were positive. Dual color fluorescence in situ hybridization was performed using a locus-specific probe(AEG1(8q22)) and a centromeric chromosome 8(CEP8) control probe. Low level gain was defined as an *AEG1*/CEP8 ratio of 1.2-2.0, while a ratio >2.0 defined an amplification. Correlations were sought between AEG1 gene copy number status, AEG1 protein expression, tumor type and overall survival. Statistical significance was determined using a Fisher exact test.
Results: The cohort included WHO grade I(10), II(6), III(13), and IV(20) gliomas. Overall 29% harbored *AEG1* copy number gains which were more frequent in high grade tumors(77%) than in low grade tumors(33%). AEG1 protein expression was present in 77% of tested gliomas, 43% of which also had *AEG1* copy number gains. Additionally, *AEG1* amplification was limited to grade III gliomas that had progressed from a low grade lesion in young patients(<30 yo) with an overall survival time >1200 days. Patients with grade III gliomas bearing *AEG1* amplification were significantly younger(p=0.002) and more likely to survive >1000 days(p=0.01694) than those with low level or no copy number gains.
Conclusions: AEG1 protein expression and/or copy number gains are present in a variety of gliomas and are more common in high grade tumors. Although AEG1 protein expression is detectable in a majority of cases, <50% harbor concomitant gene copy number gains. Of particular interest, *AEG1* amplification may be a marker of malignant progression in a subset of gliomas arising in younger patients.

1813 Targets of Differential CpG-Island Methylation in Primary vs. Recurrent Pediatric Intracranial Ependymomas

M Schniederjan, SR Williams, Y Sun, M Bouzyk, D Xie, B Rogers. Children's Healthcare of Atlanta, Atlanta, GA; Emory University, Atlanta, GA; AKESOgen Inc, Norcross, GA.
Background: Array-based platforms for genome-wide assessment of levels of CpG-island methylation provide a powerful tool to study that facet of epigenetic regulation in tumors like ependymoma. Previous reports suggest that ependymomas exhibit different patterns of methylation depending on anatomic site and other factors.
Design: To assess potential differences in patterns of CpG methylation of primary and recurrent ependymomas, we selected 22 cases of ependymoma with archived frozen tissue, five of which were recurrent, and analyzed extracted DNA for genome-wide CpG island methylation at over 450,000 loci using a commercially available bead array. We modeled beta values as the dependent variable, with the variables of recurrence as the primary independent variables in the association analysis. Linear mixed models were implemented in a multiple regression framework to adjust for the chip/positional effects of the studied samples, including age and sex as covariates. All statistical analyses were performed in the R statistical environment version 2.12.1. Because of the small sample size, only differences with p-values less than 10^{-6} were considered significant. The CpG sites were mapped to known human genes based on chromosomal location (NCBI 36.1).
Results: The results from one specimen were discarded because of a high miss rate, leaving 21 samples with data of sufficient quality. Of the methylation sites examined, three showed a difference between primary and recurrent tumors surpassing a 10^{-6} p-value. The genes associated with those sites are *MN1*, *CYP4F22,* and *ZNF846.* Six other CpG islands showed differences with p-values of 10^{-5} and were associated with *FAM47A, PLXDC1, LMF1, CORO2B, ARSH* genes.
Conclusions: Although the sample size in this series is insufficient to make inference about genome-wide patterns of methyation in primary and recurrent ependymomas, the findings suggest that there are large changes in methylation status of at least a small number of genes, some of which have been implicated in other tumor types. Whether such differences are part of the intrinsic nature of those tumors and connected with their tendency to recur or are a result of therapy, and what the functional results of those differences are, remains to be demonstrated.

1814 *BRAF*-V600E Mutation Is Rare in Gliosarcoma

KE Schwetye, DH Gutmann, S Dahiya. Washington University School of Medicine, St Louis, MO.
Background: Gliosarcoma (GS) represents a rare variant of glioblastoma (GBM), composed of both glial and mesenchymal elements. Recent studies have revealed that a small subset of GBM (epithelioid GBM) harbor *BRAF*-V600E mutations, suggesting that this mutation might predominate in specific subsets of GBM. The purpose of this study was to determine the frequency of *BRAF*-V600E mutation in GS.
Design: A search of our institutional, archival database was performed using the keyword "gliosarcoma." A total of 26 cases were reported from 1991-2012 in patients ranging in age from 29-80 years (mean = 62 years). 18 of these pathologically-verified cases were available for immunohistochemical analysis using *BRAF*-V600E-specific antibodies.
Results: A single GS tumor (1/18; ~5.6%) was focally *BRAF*-V600E-immunopositive. This particular GS contained an additional adenoid component which was positive for the mutant protein. Nine GS tumors arose in the temporal lobe, and none of these were positive for the mutant protein. The sole immunopositive tumor arose in the parietal lobe.
Conclusions: These findings demonstrate that approximately 5% of GS tumors, similar to typical GBM tumors, harbor *BRAF*-V600E mutation. It is possible that this subgroup may benefit from BRAF-targeted therapy.

1815 Clinicopathological Features and Grading in Focal Cortical Dysplasia: A Single Institutional Series

KB Urankar, T Tihan. University of California San Francisco, San Francisco, CA.
Background: The diagnostic criteria for focal cortical dysplasia have evolved over the last decade through two classification schemes known as Palmini and ILAE classifications. While both classification schemes grade many common dysplastic lesions similarly, some lesions fall into different categories. In addition, some lesions do not fit into specific grades in either scheme. The practical implications of these differences are currently unclear.
Design: We analyzed the clinicopathological features of all cases previously reported as "cortical dysplasia" in our institution between 1990 and 2013. All cases were reviewed by both authors and a consensus grading based on Palmini and ILAE classification schemes were assigned. Specific histological features in all cases were also recorded. The grading and histological features were correlated with the clinical and immunohistochemical features. Cases without sufficient pathological material and diagnoses other than focal cortical dysplasia were excluded.
Results: Among 156 cases previously reported as cortical dysplasia, we have included 92 cases in the study. There were 43 males and 49 females with a median age of 18.5 years (range: 8 months to 57 years). 39 lesions were located in the frontal lobe, 39 were in the temporal lobe, 6 were in the parietal lobe, and 8 were in the occipital lobe. According to Palmini classification, there were 8 cases in the MCD category, 13 cases in Type 1 (12- 1a, 1- 1b) category and 70 cases in Type 2 (50- 2a,20- 2b) category. Based on the ILAE classification, 17 cases were classified as Type 1 (1- 1a, no 1b, 16-1c), 55 cases were Type 2 (35- 2a, 20- 2b) and 18 cases were Type 3. 55 cases received concordant diagnoses in both schemes, while 37 cases had to be assigned to different categories in either scheme. One case could not be classified into the Palmini scheme while 2 cases did not fall into a specific category in the ILAE scheme.
Conclusions: Re-grading of focal cortical dysplasia cases needs to be performed following the introduction of the newer ILAE classification scheme, since significant number of patients would be assigned to different categories. Historical review of the literature and meta-analyses should carefully consider this significant variation before making conclusions based on the data published prior to 2011.

1816 Calvarial Fibrous Meningioma with a Reticular Growth Pattern: A Series of Seven Cases

JE Velazquez Vega, AE Rosenberg. University of Miami/Jackson Memorial Hospital, Miami, FL.
Background: Meningiomas are one of the most common tumors that arise within the central nervous system; they represent up to 30% of all intracranial tumors. Extradural meningiomas are uncommon and account for less than 2% of all meningiomas with the majority developing in the head and neck area, especially the calvarium. Meningiomas may arise de novo within the skull or may be a manifestation of direct extension from a dural-based tumor. A variety of histologic subtypes of meningioma are recognized, and we have encountered what we have classified as fibrous meningioma with a predominant reticular growth pattern in the calvarium that causes diagnostic difficulties because of its unusual morphology.
Design: We performed a search for cases of meningioma involving bone within our multi-institutional databases, as well as, from the archival consultation series of one of the authors. We examined the cases and identified the group of tumors demonstrating the pattern of interest. When available, the clinical history and imaging characteristics of the study cohort were reviewed, as well.
Results: Seven cases were identified that occurred in 6 females and 1 male, ranging in age from 56-84 years (av. 70 ± 10 yrs). Four of the patients had a previously diagnosed malignancy. Histologically, all of the tumors exhibited an infiltrative growth pattern and were composed of banal spindle cells arranged in a reticular pattern. The tumor cells formed a delicate interconnecting network that imparted a sieve-like appearance and were focally associated with abundant extracellular collagen. Focal clusters of meningothelial-type meningioma cells and whorls were seen as a minor component in several cases. There was limited cytologic atypia and little mitotic activity. Reactive woven bone formation was observed in 3 cases, and psammomatous calcifications were identified in 1 tumor. All cases were positive for EMA and PR and in the four cases tested S-100 was positive.
Conclusions: Meningioma involving the calvarium is very uncommon. We describe an infiltrating fibrous variant that because of its reticular growth pattern creates diagnostic difficulties. This is especially true in patients with a known clinical history of malignancy, and in whom metastatic disease is suspected clinically or by imaging studies. The differential diagnostic considerations include benign and malignant fibrous and fibro-osseous neoplasms, metastatic carcinoma and reactive processes. Careful histomorphological examination in conjunction with immunohistochemistry permits accurate diagnosis.

1817 Comparative Study of NF1 Copy Number Alterations in Diffuse Gliomas

MA Vizcaino-Villalobos, S Shah, FJ Rodriguez. UNAM, Mexico City, DF, Mexico; Johns Hopkins University, Baltimore, MD.
Background: Recent studies have identified somatic alterations in the gene encoding for neurofibromin (*NF1*) (mutations/deletions) in a subset of glioblastoma (GBM), usually associated with the mesenchymal molecular subtype. In the current study, we tested for *NF1* copy number alterations in a cohort of diffuse gliomas, and searched for associations with pathologic and molecular features.
Design: A cohort of 130 diffuse gliomas (11 diffuse astrocytomas (DA), 16 anaplastic astrocytomas (AA), 17 oligodendroglial tumors (OT), and 86 GBM (57 adult, 29 pediatric) were successfully evaluated for *NF1* copy number alteration using

Fluorescence in Situ Hybridization (FISH) on tissue microarrays. A custom made probe targeting the *NF1* gene (17q11.2) and a control probe targeting the centromere of Ch17 were used.

Results: *NF1*/17q or Ch 17 gains/polysomies were identified in 40/130 (31%) cases across tumors tested, including 2/11 DA, 6/16 AA, 7/17 OT and 25/86 (29%) GBM (8/29 peds-GBM, 17/57 adult GBM). However, *NF1*/17q (n=2) or whole Ch17 (n=3) losses were only identified in the GBM group (5/86 (6%)). When looking at this subset with *NF1*/Ch17 loss, the tumors were predominantly adult GBM (4/5), lacked *EGFR* amplification (0/4), strong p53 immunolabeling (1/5) or mutant IDH1 (R132H) protein expression (0/5). Conversely, the tumors expressed the mesenchymal marker podoplanin 4/5 more frequently than other diffuse gliomas 55/122(45%).

Conclusions: *NF1*/Ch17 gains occur in a subset of diffuse gliomas, irrespective of grade and pathologic subtype. Conversely, NF1/Ch17 loss identifiable by FISH is restricted to a small GBM subset, with possible unique pathologic and molecular features.

1818 Synchronous Infiltrating Gliomas with Distinct Histopathological Phenotypes and Molecular Signatures: Literature Review and Report of Two Cases

AR Wang, ZS Hoffer, CD Keene, J Zhang, DE Born, DL Silbergeld, AM Avenllino, LF Gonzalez-Cuyar. Hospital of the University of Pennsylvania, Philadelphia, PA; University of Washington, Seattle, WA.

Background: In the absence of predisposing factors like prior radiotherapy or hereditary tumor syndromes, synchronous primary intracranial tumors are exceedingly rare. While molecular diagnostic techniques may help to determine the relationship between synchronous intracranial tumors, very few reports using these techniques have been described in the literature. We present two patients with synchronous infiltrating gliomas with different histopathological phenotypes in which fluorescent in-situ hybridization (FISH) studies demonstrated co-deletions of chromosome arms 1p/19q in oligodendrogliomas, but not in their synchronous astrocytoma or mixed oligoastrocytoma.

Design: Standard hematoxylin and eosin histology, immunohistochemistry, and fluorescent in situ hybridization (FISH) on formalin fixed paraffin embedded tissue sections were used to characterize the histopathologic, immunohistochemical, and molecular signatures of the resected infiltrating gliomas in each patient.

Results: The first patient had two masses: a GFAP-positive mitotically active right frontal anaplastic oligodendroglioma (WHO Grade III) with 1p/19q codeletions, and a GFAP-positive mitotically active right temporal mixed anaplastic oligoastrocytoma (WHO Grade III) polysomic for chromosome arms 1p and 19q. The second patient had three masses: a p53-positive mitotically active right frontal anaplastic astrocytoma (WHO Grade III) without 1p or 19q deletions, a mitotically quiescent 1p/19q codeleted right superolateral temporal oligodendroglioma, and a polysomic mitotically quiescent GFAP-positive right mesial temporal diffuse astrocytoma (WHO Grade II).

Conclusions: This report expands the narrow literature of synchronous infiltrating glial neoplasms with unique molecular signatures, and when compiled with other similar reports of synchronous gliomas, should help elucidate unique diagnostic, prognostic, and therapeutic approaches for dealing with patients with synchronous infiltrating gliomas.

1819 IDH1 Mutation Is Associated with Decreased Proliferative Activity in Newly Diagnosed Anaplastic Gliomas

JK Wasserman, G Jansen, R Yaworski, J Woulfe. University of Ottawa, Ottawa, ON, Canada.

Background: Anaplastic glioma is a high-grade primary brain tumor that invariably progresses to glioblastoma. Previous studies have shown that tumors harbouring a mutation in the isocitrate dehydrogenase-1 (IDH1) gene have a better prognosis than patients with wild-type tumors. Why IDH mutant tumors behave less aggressively is a subject of intensive research. Proliferative activity is an indicator of increasing malignancy although it is not known whether IDH1-positive and wild-type tumors differ in this regard. We hypothesized that wild-type tumors would be more proliferative and that the higher rate of proliferation would be associated with early progression to glioblastoma.

Design: Patients diagnosed with anaplastic astrocytoma or oligoastrocytoma were included in this study; anaplastic oligodendrogliomas and tumors arising from a low grade (WHO grade II) precursor were excluded. Immunohistochemistry was used to determine mutation status and proliferative activity using antibodies specific for the IDH1 R132H mutation and Ki-67, respectively. Mitotic activity was graded as low ($\leq$ 5 mitotic figures / mm^2) or high (> 5 mitotic figures / mm^2). Progression-free survival was assessed 12 months after the initial diagnosis.

Results: A total of 37 anaplastic gliomas were studied; 18 (49%) were IDH1 mutation positive. Patients whose tumors were IDH1-positive tended to be younger than patients with IDH wild-type tumors (44.2 ± 16.5 vs. 55.2 ± 17.2) although the difference was not significant ($p > 0.05$). Proliferative activity as measured by the Ki-67 labelling index was significantly higher in IDH1 wild-type tumors compared to IDH-mutant tumors (23.8 ± 14.7% vs. 13.8 ± 10.5%; p=0.02). In contrast, the proportion of tumors with high mitotic activity did not differ between IDH1-positive and IDH1 wild-type tumors (0.39 vs. 0.42; $p > 0.05$). Seven patients (39%) with IDH1-positive tumors and 10 (53%) with IDH wild-type tumors experienced disease progression within 12 months of their initial diagnosis ($p > 0.05$). Proliferative activity did not differ significantly between patients who experienced disease progression and those who remained progression-free (23.0 ± 16.8% vs. 15.5 ± 0.9%; $p > 0.05$).

Conclusions: Anaplastic gliomas that possess the IDH1 mutation have decreased proliferative activity compared to wild-type tumors which may explain why these tumors are associated with improved long-term prognosis. A better understanding of the cellular mechanisms responsible for restricting proliferation in IDH1-positive tumors may translate into strategies for controlling tumor growth.

1820 Solid Nonhematopoietic CNS Metastases in the Pediatric Population: 30-Year Neuropathologic Experience at a Large Regional Children's Hospital

AL Wiens, EM Hattab. Indiana University School of Medicine, Indianapolis, IN.

Background: Collectively, metastatic tumors are the most common malignancy encountered in the adult central nervous system (CNS), arising most often from cancers of the lung, breast, skin, and gastrointestinal tract. Limited information is available in the literature regarding solid nonhematopoietic CNS metastases in children.

Design: We carried out a 30-year retrospective study of metastatic neoplasms to the CNS in the pediatric population to characterize their frequency, common histologic subtypes, and sites of origin. Archival pathology files at Riley Hospital for Children and its affiliated hospitals were searched (1981–2011) for metastatic tumors to the CNS in patients 21 years of age and younger. Pathology material was reviewed, tumors were classified by site of origin and histologic subtype, and survival was evaluated.

Results: We identified 26 patients with solid nonhematopoietic CNS metastases out of 1135 pediatric CNS tumors diagnosed from 1981–2011. Patients ranged from 1.5–20.3 years (mean, 10.7; median, 10.6 years) and were equally divided between genders (13 male, 13 female). Most CNS metastases were supratentorial (85%) and solitary (65%). Mean interval from primary malignant diagnosis to CNS metastasis was 27 months (median, 18 months). Sites of origin included kidney/adrenal, bone/soft tissue, gonads, head and neck, lung, and liver. Mean survival after CNS involvement was 36.6 months (median, 12.5 months). Overall 1-year and 5-year survival rates were 52% and 16%, respectively.

Conclusions: In neuropathology practice, nonhematopoietic pediatric CNS metastases are far less common than those of the adult population, accounting for approximately 2% of all pediatric CNS tumors. The most common tumors to exhibit CNS metastasis are of kidney/adrenal origin, followed by those from bone/soft tissue. As expected, prognosis is dismal, despite aggressive therapy.

1821 Molecular Alterations in Melanoma Metastases to the Central Nervous System and Their Clinicopathologic Relevance

I Yilmaz, M Gamsizkan, T Tihan. GATA Haydarpasa Training Hospital, Istanbul, Turkey; Erzurum Military Hospital, Erzurum, Turkey; UCSF, School of Medicine, San Francisco, CA.

Background: Melanoma is among the most common malignancies that metastasize to the central nervous system (CNS). The molecular characteristics of primary melanomas have been used to either diagnose an undifferentiated metastatic tumor as origination from a melanoma, or to develop targets for chemotherapy. In certain instances, such analyses may utilize immunohistochemical markers to determine the presence or absence of a mutation that constitutes a treatment target.

Design: We aimed to analyze the genetic alterations in 48 patients with CNS metastatic melanomas and to compare these analyses with clinical and pathological findings to determine 1) diagnostically relevant alterations, 2) validation of putative chemotherapy targets. For mutation analysis, tumor targets were microdissected from unstained histological sections and DNA's were isolated from each target. Exon 15 of BRAF gene, exon 9, 11, 13, 17 and 18 of c-kit gene, exon 2 and 3 of NRAS gene, exon 4 and 5 of GNAQ and GNA11 gene mutations were analyzed using PCR based direct sequencing. After purification of PCR products, the amplicons were submitted to direct sequencing in both directions using reagents from the Big Dye Terminator kit and analyzed in the ABI 3730 automatic sequencer. Immunohistochemical studies for c-kit and other markers were performed with the standard methodology at our institution.

Results: PCR was successful in 47 of 48 cases. BRAF-exon 15 was noted as the most common mutation (27/46; 58.7%). NRAS-exon 3 mutation was detected in 7 cases, NRAS-exon 2 mutation was identified in 3, GNAQ-exon 5 and GNA11-exon 5 mutation were in one tumor each. None of the tumors had GNAQ-exon 4 mutation. Most female patients had BRAF mutations (p=0.009), while others were more common in males (p=0.024). While focal or strong c-kit immunopositivity was observed in 33 cases, only one tumor showed a mutation in c-kit-exon 11 (c.1727T>C; p.L576P; Substitution-Missense).

Conclusions: The distribution of mutations in metastatic melanomas seems to be different among genders. C-kit immunohistochemistry is not a good predictor of the presence of molecular mutations, and activating mutations are rare in CNS metastatic melanoma. Studies are under way to determine differences between primary tumors and their metastases in terms of these genetic alterations.

1822 T-Cell Lymphoma Presenting as Benign Idiopathic Perineuritis

J Ziskin, H Vogel. Stanford University, Palo Alto, CA.

Background: Perineuritis involving peripheral nerves has diverse causes, including infectious, sarcoidosis, toxic, and paraneoplastic etiologies.

Design: We report an example of disseminated peripheral and presumed cranial nerve involvement by T-cell lymphoma without extraneural disease at presentation. A 31 year old female developed Bell's palsy affecting her right face. Two months later, she developed distal leg paresthesias which spread proximally, progressing to upper extremity involvement one month later. She was hospitalized because of worsening weakness and underwent normal CSF examination, and positive MRI showing spinal C6 root and right brachial plexus enlargement. Bone marrow biopsy showed leukopenia and a left shift by flow cytometry. Extensive infectious and rheumatological evaluations were negative. A left gastrocnemius biopsy and sural nerve biopsy were performed.

Results: A nongranulomatous infiltrate of the nerve by small lymphocytes without atypicality was noted, with acute denervation atrophy of the muscle. Immunophenotyping for B and T-cell markers showed a near-100% predominance of CD3+ lymphocytes. A diagnosis of idiopathic perineuritis was made. The patient underwent plasmapheresis, corticosteroid, and cyclophosphamide therapy with stabilization of the signs of

peripheral neuropathy. 2 months later a thigh mass developed. Biopsy showed peripheral T-cell lymphoma, CD3+, CD4+, CD5+, CD56+, PD-1+, T-cell intracellular antigen-1 (TIA-1)+ and TCR-beta+, and CD30-, TdT-, CD34-, CD138-, and CD21-. Rare cells were CD8+ and CD20+, and positive for TCR gamma gene rearrangement by PCR. The sural nerve biopsy showed additional immunopositivity for CD4, CD56, and TIA-1, matching the thigh mass lymphoma immunophenotype.
Conclusions: T-cell lymphoma of peripheral nerves has been described as a solitary mass of the median nerve and in the presence of widely disseminated lymphoma. We demonstrate for the first time the utility of aberrant CD56 and TIA-1 immunopositivity in diagnosing lymphomatous neuropathy. This case also draws attention to several other reports of apparently benign lymphocytic infiltrates affecting nerves in systemic non-Hodgkin lymphomas may in fact represent lymphomatous involvement of nerve.

Ophthalmic Pathology

1823 Clinicopathologic Features of Orbital Space-Occupying Lymphoid Lesions: A Single Institution Experience

J Boone, F Fan. University of Kansas Medical Center, Kansas City, KS.
Background: Lymphoid-rich lesions compose a large proportion of space-occupying lesions of the orbit. Differential diagnoses include infectious, inflammatory/reactive, autoimmune and neoplastic processes. It poses diagnostic challenge to pathologists due to limited biopsy material and often times overlapping histologic features. Current literature on this subject is comprised of mostly case reports. This study is designed to collect clinicopathological data on lymphoid space occupying lesions of the orbit in our hospital.
Design: A list of patients diagnosed with a lymphoid infiltrative lesion of the orbit was obtained from the surgical pathology specimen records. The reports were reviewed and histologic data including diagnosis, immunohistochemical staining, flow cytometry, and molecular testing were recorded. The cases were divided into four categories as: reactive/inflammatoy, IgG4 related sclerosing dacryoadenitis, atypical lymphoid infiltrate and lymphoma. The critical ancillary test that led to the final diagnosis was identified. Pertinent clinical information were also collected.
Results: There were a total of 44 cases over an eleven-year period in our institution. The majority of cases (88.6%) represented a primary disease process in the orbital region. Male to female ratio was 2:1 and the age range was 31-98 years old. Among the 44 cases, 22 cases were reactive/inflammatory (50%), 2 were IgG4 related disease (4.5%), 6 were atypical lymphoid infiltrate (13.6%), and 14 were lymphoma (31.8%). All lymphoma cases were B-cell lymphomas with extranodal marginal zone lymphoma being the most common (57.1%) type, followed by follicular lymphoma, diffuse large B-cell lymphoma and mantle cell lymphoma. Ancillary testing (immunohistochemical staining, flow cytometry and gene rearrangement) was used in 81% of cases to reach a final diagnosis. Among them, flow cytometry was identified to be the critical ancillary test most frequently.
Conclusions: Orbital space-occupying lymphoid lesions are rare overall. Most are primary orbital lesions with half being benign reactive/inflammatory process. The second most common lesion is B-cell lymphoma. IgG4 related sclerosing disease makes only a small portion of cases. Flow cytometry appears to be the most useful test in the work-up of orbital lymphoid lesions and should be considered a priority in cases with limited tissue size.

1824 Clinicopathologic Correlations in 2,487 Consecutive Corneal Specimens from a Single Ophthalmic Pathology Laboratory

YJ Cruz-Inigo, DO Hodge, JJ Garcia, SV Patel, DR Salomao. Mayo Clinic, Rochester, MN.
Background: Corneal specimens are unfamiliar to a general surgical pathologist. Biopsies are performed to exclude infectious processes and resections to treat generalized corneal diseases and correct optical consequences. We reviewed clinical and pathological records of all corneal specimens submitted to our laboratory to determine differences between intramural (in-house), extramural (consultation) specimens, and trends over time.
Design: Retrospective search of surgical pathology database for all corneal specimens submitted from January 1994 to July 2012. Reports were evaluated for patients' demographics, clinical indications, procedure type and histopathological interpretation. Statistical analysis was performed.
Results: Study cohort comprised of 2,487 specimens from 2,011 patients: 887 males (44%) and 1,124 females (56%); mean age 64 yrs (median 70 yrs; range 2 mos-102 yrs); 50% from right, 47% from left, and 3% undesignated. Most were intramural specimens (61%); penetrating (73%) or lamellar keratoplasties (19%), and corneal biopsies (9%). Multiple specimens on a single patient were intramural cases only (24%). Statistical analysis showed percentage of intramural and extramural penetrating keratoplasties decreased ($p<0.001$) and lamellar keratoplasties increased ($p<0.001$) over time. Percentage of corneal biopsies, intramural ($p=0.36$) and extramural ($p= 0.16$), remained constant. Most frequent pathologic diagnoses were Fuchs' dystrophy (27%), bullous keratopathy (18%), keratoconus (16%), graft failure (10%) and corneal scarring (9%). Comparison between intramural and extramural cases revealed that Fuchs' dystrophy (33% vs 17%; $p<0.001$) and corneal ulceration (6% vs 3%; $p=0.003$) were more often diagnosed in intramural specimens, while graft failure (13% vs 19%; $p<0.001$) and degenerations (1% vs 3%; $p<0.001$) were more often in extramural specimens. On trend analysis, the percentage of intramural procedures performed for Fuchs' dystrophy ($p=0.007$) and graft failure ($p<0.001$) increased over time; same was observed for graft failure ($p=0.008$) and scarring ($p=0.002$) on extramural specimens. Bullous keratopathy decreased over time in the latter group ($p<0.001$).
Conclusions: Our study confirms a trend in surgical treatment of corneal diseases; lamellar keratoplasty is becoming more common in both intramural and extramural practices. In this series, most common diagnoses were Fuchs' dystrophy, bullous keratopathy, keratoconus and graft failure. The latter diagnosis has increased over time in both intramural and extramural specimens.

1825 Adenoid Cystic Carcinoma of the Lacrimal Gland Is Frequently Characterized by t(6;9) and May Be Distinguished from Other Neoplasms Using Fluorescent In Situ Hybridization

MG Keeney, WR Sukov, JA Garrity, DR Salomao, JJ Garcia. Mayo Clinic, Rochester, MN.
Background: Adenoid cystic carcinoma (ACC) of the lacrimal gland is a rare tumor that is almost universally fatal. ACC is composed of a dual cell population (ductal and myoepithelial cells) and may demonstrate tubular, cribriform, and/or solid architectural patterns. Unfortunately, these histopathologic features are not specific to ACC and can be seen in other lacrimal gland neoplasms, occasionally posing a diagnostic dilemma. Although t(6;9)(q22-23;p23-24), involving *MYB* and *NFIB,* has been identified in a significant portion of ACC cases arising from other anatomic sites, its role in the pathogenesis of lacrimal gland ACC has not been elucidated. This study explores the incidence of t(6;9) in ACC arising from the lacrimal gland, and the diagnostic utility of fluorescence *in situ* hybridization (FISH) in the clinical setting.
Design: Retrospective clinical and histopathologic review of 6 cases of lacrimal gland ACC seen at Mayo Clinic over a 14-year period (1998-2012) was performed. Clinical data including patient age, sex, tumor size, treatment (surgery, radiotherapy, and/or chemotherapy), and clinical outcome parameters were obtained from medical records when available. Surgical pathology archival material was re-examined and formalin-fixed paraffin-embedded (FFPE) material was further evaluated with IHC when appropriate. FFPE material from all 6 cases and normal controls was assessed with FISH using a *MYB* break-apart probe designed and validated for clinical use.
Results: The median patient age was 59.5 years (range 25-75) and 4 patients were male (67%). Rearrangement of *MYB* was identified using FISH in 3 cases (50%) while normal controls showed no evidence of *MYB* rearrangement. No correlation between *MYB* rearrangement and histopathologic features, disease-specific, or overall survival was observed.
Conclusions: These study results show that t(6;9) is a frequent event in lacrimal gland ACC. The incidence of MYB rearrangement in lacrimal gland ACC rivals that of ACC arising from other anatomic sites—approximately 50%. To this end, FISH for *MYB* rearrangement may be used as a diagnostic tool when the diagnosis of ACC of the lacrimal gland is in question. Lastly, the presence of t(6;9) in ACC may provide a platform for molecular targeting strategies in the future.

1826 Investigation of C-MET in Uveal Melanoma

SM Kennedy, C Barr, M Clynes, A Larkin. Royal Victoria Eye and Eye and Ear Hospital, Dublin 4, Ireland; National Institute for Cellular Biotechnology, Dublin City University, Dublin 9, Ireland.
Background: Uveal melanoma is the most common primary intraocular neoplasm affecting adults, over 50% of patients develop incurable metastatic disease. There is an urgent need to develop effective therapies for metastatic uveal melanoma. Altered c-MET signalling is known to be involved in uveal melanoma progesssion. The mechanism of cMET activation is unknown. Selective MET inhibition has been suggested as a potentially useful therapeutic target in uveal melanoma. Significantly lower BRAF mutation rates and increased rates in c-MET mutations have recently been reported in Irish patients with cutaneous melanoma (1). The aim of this retrospective study was to investigate c-MET activation in Irish patients diagnosed with uveal melanoma.
Design: Expression of cMET and activated phospho cMET was studied using Immuncytochemistry on TMAs from 192 enucleated tumours from Irish patients (86 female, 104 male) diagnosed with uveal melanoma with minimum 10 year follow-up. The study group included 78 spindle, 25 epitheloid and 84 mixed cell type tumours, 45% of this cohort developed metastasis and died of disease. cMET immunoreactivity was scored as zero, weak (1), intermediate (2) or strong (3) based on the intensity of the staining observed.
Results: Total cMET staining was predominantly cytoplasmic, with some weak membrane positivity observed. cMET was positive in 152 (79%) of tumours, with strong staining observed in 21 (10%), intermediate staining in 62 (33%) and weak staining in 36% of tumours. Strong c-MET immunoreactivity was associated with epithelioid type tumours and a higher percentage of tumours which showed metastasis exhibited strong c-MET immunoreactivity compared to tumours without metastasis. Phospho cMET immunostaining has been optimised in cutaneous melanoma tumours, phospho cMET expression in this uveal melanoma patient cohort will be correlated with clinicopathological features of patients.
Conclusions: c-MET is highly expressed in Irish uveal melanoma patients; strong cMET immunoreactivity is associated with epithelioid tumour cell type and metastasis indicating that high c-MET expression is associated with adverse outcome. The results of this study will provide important information regarding the incidence of phospho activated cMET in Irish uveal melanoma patients, and will have implications for potential development of cMET as a potential therapeutic target for the treatment of metastatic uveal melanoma in the Irish population.
1 Gallagher WM, AACR 2013 (Abstract).